

Four-nucleon force using the method of unitary transformation

E. Epelbaum^{1,2,*}¹*Forschungszentrum Jülich, Institut für Kernphysik (Theorie), D-52425 Jülich, Germany*²*Universität Bonn, Helmholtz-Institut für Strahlen- und Kernphysik (Theorie), D-53115 Bonn, Germany*

(Dated: September 15, 2021)

We discuss in detail the derivation of the leading four-nucleon force in chiral effective field theory using the method of unitary transformation. The resulting four-nucleon force is given in both momentum and configuration space. It does not contain any unknown parameters and can be used in few- and many-nucleon studies.

PACS numbers: 21.45.+v, 21.30.-x, 25.10.+s

I. INTRODUCTION

Chiral effective field theory (EFT) is a powerful tool for analyzing the properties of hadronic systems at low energies in a systematic and model-independent way. It exploits the approximate and spontaneously broken chiral symmetry of QCD which governs low-energy hadron structure and dynamics. Over the past years, considerable progress has been achieved in understanding the structure of the nuclear force in this framework, see [1, 2] for recent review articles. In particular, two-nucleon force (2NF) has been worked out and applied in few-nucleon studies upto next-to-next-to-next-to-leading (N^3LO) in the chiral expansion [3, 4]. Three-nucleon force is currently available at next-to-next-to-leading order (N^2LO) [5, 6], see [7, 8, 9] for some examples of recent few-nucleon studies at N^2LO . Although the results for most of the investigated few-nucleon observables look promising, it is necessary to go to N^3LO in order to test the convergence of the chiral expansion. Increasing the chiral order is also expected to bring new insights into certain existing puzzles in the 3N continuum such as e.g. the large deviations from the data for the differential cross section in some deuteron breakup configurations, see [10] for a recent work on this subject. The full N^3LO analysis requires the incorporation of the subleading contributions to the 3NF which are currently being worked out. In addition, one has to take into account four-nucleon force (4NF) which starts to contribute at this order. In Ref. [11] we already presented the expressions for the leading 4NF. It is governed by the exchange of pions and the lowest-order nucleon-nucleon contact interaction and includes effects due to the nonlinear pion-nucleon couplings and the pion self-interactions constrained by the chiral symmetry of QCD. The obtained 4NF is local and does not contain any unknown parameters. In this work, we describe in detail the derivation of the 4NF using the method of unitary transformation [12, 13], for which a new formulation is presented. This new formulation is considerably simpler than the one given in Refs. [12, 13] and much more convenient for practical applications. We furthermore study the effects of the additional unitary transformations which affect the form of the effective Hamilton operator at N^3LO . The appearance of such transformations is a new feature at this order in the chiral expansion.

Our manuscript is organized as follows. In section II we discuss the chiral power counting in the few-nucleon sector following the original formulation by Weinberg [14, 15]. We express the power of the low-momentum scale in a different form as compared to Refs. [14, 15] which is particularly useful for applications based on algebraic rather than diagrammatic methods. Combining this new formulation with the method of unitary transformation we obtain the formal expression for the effective nuclear Hamilton operator in a compact form. In section III we use this new formulation to derive the N^3LO contributions to the effective nuclear Hamiltonian and evaluate the corresponding four-nucleon operators which give rise to the 4NF. We employ a large class of additional unitary transformations acting on the nucleon subspace of the full Fock space and investigate their impact on 3NFs and 4NFs. We end with the summary and outlook. Finally, appendix A contains some details related to the N^3LO contributions involving subleading vertices while the expressions for the 4NF in configuration space are given in appendix B.

*Email: e.epelbaum@fz-juelich.de

II. NUCLEAR FORCES IN CHIRAL EFT USING THE METHOD OF UNITARY TRANSFORMATION

A. Chiral power counting

Power counting is a crucial ingredient of any effective field theory which allows to organize various contributions to the scattering amplitude according to their relevance. Throughout this work, we adopt Weinberg's power counting which is based on naive dimensional analysis¹. Traditionally, chiral power counting is formulated in terms of topological quantities such as the number of loops and, in the few-nucleon sector, the number of participating nucleons and disconnected pieces [14, 15, 16]. This allows to immediately identify all relevant diagrams at a given order and appears to be particularly useful for calculations based on the Feynman graph technique. For algebraic approaches such as the method of unitary transformation [12, 13] it is more convenient to express the power counting in a different form which will be given below. For the sake of completeness, let us first recall the derivation of Weinberg's power counting result following his original work [14, 15]. Consider an arbitrary N -nucleon irreducible time-ordered diagram (i.e. the one that does not contain iterative contributions) without external pions. For the sake of generality, we allow for cases in which \tilde{N} out of N nucleons do not interact. To obtain the corresponding power ν of the soft scale Q one has to count the number of the independent three-dimensional momentum-space integrations $I - \sum_i V_i$ with I (V_i) being the number of internal lines (vertices of type i), the number d_i of derivatives or pion mass insertions at each vertex, the number D of energy denominators and the number of phase-space factors associated with exchanged pions:

$$\nu = 3I - 3 \left(\sum_i V_i - 1 \right) - D + \sum_i V_i \left(d_i - \frac{p_i}{2} \right) - 3\tilde{N}. \quad (2.1)$$

Here, p_i denotes the number of pion fields at a vertex of type i . Notice that we follow the standard convention to define the potential. In particular, we do not count the overall δ -function that enters the definition of the S-matrix element but do count the additional δ -functions associated with the noninteracting nucleons. To bring Eq. (2.1) into the standard form one can use the following topological identities. First, the number of intermediate states D can be expressed as:

$$D = \sum_i V_i - 1. \quad (2.2)$$

Secondly, the number of loops L is given by

$$L = I - \sum_i V_i + C - \tilde{N}, \quad (2.3)$$

where C refers to the number of separately connected pieces. Notice that each noninteracting nucleon is regarded as a separately connected piece. The last identity we need reads

$$2I + 2N = \sum_i V_i (p_i + n_i) + 2\tilde{N}. \quad (2.4)$$

Here, n_i is the number of nucleon field operators at a vertex of type i . Using Eqs. (2.2), (2.3) and (2.4), one can rewrite Eq. (2.1) in the form that appears in Weinberg's original papers [14, 15, 17]:

$$\nu = 4 - N + 2(L - C) + \sum_i V_i \Delta_i, \quad \Delta_i = d_i + \frac{1}{2}n_i - 2. \quad (2.5)$$

There is one subtlety in the above expression which needs to be addressed: according to Eq. (2.5), the chiral dimension ν for a given process depends on the total number of nucleons in the system. For example, one-pion exchange in the two-nucleon system corresponds to $N = 2$, $L = 0$, $C = 1$ and $\sum_i V_i \Delta_i = 0$ and, therefore, contributes at order $\nu = 0$. On the other hand, the same process in the presence of the third (spectator) nucleon leads, according to Eq. (2.5), to

¹ Notice that alternative counting schemes for contact two-nucleon interactions are currently being explored.

$\nu = -3$ since $N = 3$ and $C = 2$. The origin of this discrepancy lies obviously in the different normalization of the 2N and 3N states:

$$\begin{aligned} 2N : \quad & \langle \vec{p}_1 \vec{p}_2 | \vec{p}_1' \vec{p}_2' \rangle = \delta^3(\vec{p}_1' - \vec{p}_1) \delta^3(\vec{p}_2' - \vec{p}_2), \\ 3N : \quad & \langle \vec{p}_1 \vec{p}_2 \vec{p}_3 | \vec{p}_1' \vec{p}_2' \vec{p}_3' \rangle = \delta^3(\vec{p}_1' - \vec{p}_1) \delta^3(\vec{p}_2' - \vec{p}_2) \delta^3(\vec{p}_3' - \vec{p}_3). \end{aligned} \quad (2.6)$$

It can be circumvented by assigning a chiral dimension to the transition operator rather than to its matrix elements in the N -nucleon space. Adding the factor $3N - 6$ to the right-hand side of Eq. (2.5) in order to account for the normalization of the N -nucleon states and to ensure that the LO contribution to the nuclear force appears at order $\nu = 0$ we obtain

$$\nu = -2 + 2N + 2(L - C) + \sum_i V_i \Delta_i. \quad (2.7)$$

We will now rewrite this expression in a different form which is better suited for the method of unitary transformation. To that aim we combine Eqs. (2.3) and (2.4) and express $2(L - C)$ as

$$2(L - C) = -2N + \sum_i V_i (p_i + n_i - 2). \quad (2.8)$$

Substituting this expression into Eq. (2.7) leads to

$$\nu = -2 + \sum_i V_i \kappa_i, \quad \kappa_i = d_i + \frac{3}{2}n_i + p_i - 4. \quad (2.9)$$

Clearly, the quantity κ_i which enters this expression is just the canonical field dimension of a vertex of type i (up to the additional constant -4) and gives the inverse mass dimension of the corresponding coupling constant. It should further be emphasized that Eq. (2.9) can be obtained immediately by counting inverse powers of the hard scale Λ rather than powers of the soft scale Q (which is, of course, completely equivalent). Indeed, since the only way for the hard scale to be generated is through the values of the low-energy constants (LECs), the power ν is just the negative of the overall mass dimension of all LECs. The additional factor -2 in Eq. (2.9) is a convention to ensure that the contributions to the nuclear force start at $\nu = 0$. While Eq. (2.9) does not say much about the topology and is, therefore, not particularly useful to deal with diagrams, it is very convenient for algebraical calculations. In particular, it allows to (formally) reduce the chiral expansion to the ordinary expansion in powers of the coupling constant. The role of the coupling constant is played by the ratio Q/Λ , and the power of the coupling constant for a vertex of type i is given by κ_i . Clearly, for perturbation theory to be applicable it is necessary, that only nonrenormalizable (i.e. the ones with $\kappa_i > 0$) interactions appear in the Lagrangian. This is guaranteed by the spontaneously broken chiral symmetry.

B. Application to the method of unitary transformation

We are now in the position to apply Eq. (2.9) to derive nuclear forces from the effective chiral Lagrangian using the method of unitary transformation. The starting point is the time-independent Schrödinger equation for interacting pions and nucleons

$$(H_0 + H_I)|\Psi\rangle = E|\Psi\rangle, \quad (2.10)$$

where $|\Psi\rangle$ denotes an eigenstate of the Hamiltonian H with the eigenvalue E . Let η (λ) be projection operators onto the purely nucleonic (the remaining) part of the Fock space satisfying $\eta^2 = \eta$, $\lambda^2 = \lambda$, $\eta\lambda = \lambda\eta = 0$ and $\lambda + \eta = \mathbf{1}$. To study nuclear systems below the pion production threshold it is advantageous to project Eq. (2.10) onto the η -subspace of the full Fock space. The resulting effective equation can then be solved using the standard methods of few- or many-body physics. This reduction can be achieved via an appropriately chosen unitary transformation

$$\tilde{H} \equiv U^\dagger H U = \begin{pmatrix} \eta \tilde{H} \eta & 0 \\ 0 & \lambda \tilde{H} \lambda \end{pmatrix}. \quad (2.11)$$

Following Okubo [18], the unitary operator U can be parametrized as

$$U = \begin{pmatrix} \eta(1 + A^\dagger A)^{-1/2} & -A^\dagger(1 + AA^\dagger)^{-1/2} \\ A(1 + A^\dagger A)^{-1/2} & \lambda(1 + AA^\dagger)^{-1/2} \end{pmatrix}, \quad (2.12)$$

with the operator $A = \lambda A \eta$. The operator A has to satisfy the decoupling equation

$$\lambda(H - [A, H] - AHA)\eta = 0 \quad (2.13)$$

in order for the transformed Hamiltonian \tilde{H} to be of a block-diagonal form. The effective η -space potential V can be expressed in terms of the operator A as:

$$V = \eta(\tilde{H} - H_0) = \eta \left[(1 + A^\dagger A)^{-1/2} (H + A^\dagger H + HA + A^\dagger HA) (1 + A^\dagger A)^{-1/2} - H_0 \right] \eta. \quad (2.14)$$

The potential V can be derived perturbatively based on the chiral power counting. In Refs. [12, 13] this was achieved using Eq. (2.7) via a two-dimensional recursive process which required rather tedious calculations in the intermediate steps. As an alternative, one can use Eq. (2.9) to express H_I as

$$H_I = \sum_{\kappa=1}^{\infty} H^\kappa \quad (2.15)$$

with κ being defined in Eq. (2.9). Assuming the following expansion for the operator A

$$A = \sum_{\kappa=1}^{\infty} A^\kappa, \quad (2.16)$$

one immediately obtains from Eq. (2.13):

$$A^\kappa = \frac{1}{E_\eta - E_\lambda} \lambda \left\{ H^\kappa + \sum_{i=1}^{\kappa-1} H^i A^{\kappa-i} - \sum_{i=1}^{\kappa-1} A^{\kappa-i} H^i - \sum_{i=1}^{\kappa-2} \sum_{j=1}^{\kappa-i-1} A^i H^j A^{\kappa-i-j} \right\} \eta. \quad (2.17)$$

Here, E_η (E_λ) refers to the free energy of nucleons (nucleons and pions) in the state η (λ). The expression for the effective potential follows immediately by substituting Eqs. (2.15) and (2.17) into Eq. (2.14).

III. DERIVATION OF THE LEADING FOUR-NUCLEON FORCE

A. Effective Lagrangian

The effective chiral Lagrangian for pions and nucleons has the form, see e.g. [19, 20]:

$$\begin{aligned} \mathcal{L}_{\pi\pi} &= \frac{F_\pi^2}{4} \text{tr} [\partial_\mu U \partial^\mu U^\dagger + M_\pi^2 (U + U^\dagger)] + \dots, \\ \mathcal{L}_{\pi N} &= N^\dagger \left(iD_0 - \frac{g_A}{2} \vec{\sigma} \cdot \vec{u} \right) N + \dots, \\ \mathcal{L}_{NN} &= -\frac{1}{2} C_S (N^\dagger N) (N^\dagger N) - \frac{1}{2} C_T (N^\dagger \vec{\sigma} N) \cdot (N^\dagger \vec{\sigma} N) + \dots, \end{aligned} \quad (3.18)$$

where only those terms are shown explicitly which contribute to the leading 4NF. Here, $F_\pi = 92.4$ MeV ($g_A = 1.267$) is the pion decay constant (the nucleon axial-vector coupling), N represents a non-relativistic nucleon field and $\vec{\sigma}$ denote the Pauli spin matrices. The low-energy constants C_S and C_T determine the strength of the leading NN short-range interaction [14, 15]. Further, the SU(2) matrix $U = u^2$ collects the pion fields, $D^\mu = \partial^\mu + \frac{1}{2}[u^\dagger, \partial^\mu u]$ denotes the covariant derivative of the nucleon field and $u_\mu = iu^\dagger \partial_\mu U u^\dagger$. The first terms in the expansion of the matrix $U(\boldsymbol{\pi})$ in powers of the pion fields take the form

$$U(\boldsymbol{\pi}) = 1 + \frac{i}{F_\pi} \boldsymbol{\tau} \cdot \boldsymbol{\pi} - \frac{1}{2F_\pi^2} \boldsymbol{\pi}^2 - \frac{i\alpha}{F_\pi^3} (\boldsymbol{\tau} \cdot \boldsymbol{\pi})^3 + \frac{8\alpha - 1}{8F_\pi^4} \boldsymbol{\pi}^4 + \dots, \quad (3.19)$$

where $\boldsymbol{\tau}$ denote the Pauli isospin matrices and α is an arbitrary constant. Notice that only the coefficients in front of the linear and quadratic terms in the pion field are fixed uniquely from the unitarity condition $U^\dagger U = 1$ and the

proper normalization of the pion kinetic energy. The explicit α -dependence of the matrix U represents the freedom in the definition of the pion field. Clearly, all measurable quantities are α -independent.

Expanding the terms in Eq. (3.18) in powers of pion fields and applying the canonical formalism leads to the following interaction terms in the Hamilton density:

$$\begin{aligned}
\mathcal{H}^1 &= \frac{g_A}{2F_\pi} N^\dagger \boldsymbol{\tau} \vec{\sigma} \cdot \vec{\nabla} \boldsymbol{\pi} N, \\
\mathcal{H}^2 &= \frac{4\alpha - 1}{2F_\pi^2} (\boldsymbol{\pi} \cdot \partial_\mu \boldsymbol{\pi})^2 + \frac{\alpha}{F_\pi^2} \boldsymbol{\pi}^2 (\partial_\mu \boldsymbol{\pi} \cdot \partial^\mu \boldsymbol{\pi}) - \frac{8\alpha - 1}{8F_\pi^2} M_\pi^2 \boldsymbol{\pi}^4 + \frac{1}{4F_\pi^2} N^\dagger \boldsymbol{\tau} \cdot (\boldsymbol{\pi} \times \dot{\boldsymbol{\pi}}) N \\
&\quad + \frac{1}{2} C_S (N^\dagger N) (N^\dagger N) + \frac{1}{2} C_T (N^\dagger \vec{\sigma} N) \cdot (N^\dagger \vec{\sigma} N), \\
\mathcal{H}^3 &= -\frac{g_A}{2F_\pi^3} N^\dagger \left[\left(2\alpha - \frac{1}{2} \right) (\boldsymbol{\tau} \cdot \boldsymbol{\pi}) (\boldsymbol{\pi} \vec{\sigma} \cdot \vec{\nabla} \boldsymbol{\pi}) + \alpha \boldsymbol{\pi}^2 (\boldsymbol{\tau} \vec{\sigma} \cdot \vec{\nabla} \boldsymbol{\pi}) \right] N, \\
\mathcal{H}^4 &= \frac{1}{2(2F_\pi)^2} [N^\dagger (\boldsymbol{\tau} \times \boldsymbol{\pi}) N] \cdot [N^\dagger (\boldsymbol{\tau} \times \boldsymbol{\pi}) N].
\end{aligned} \tag{3.20}$$

Here, the superscripts of \mathcal{H} refer to the canonical field dimension κ defined in Eq. (2.9). Again, we only show those terms in the Hamilton density which are relevant for the present calculation. Notice that the last term in Eq. (3.20) is absent in the effective Lagrangian in Eq. (3.18) and arises through the application of the canonical formalism, see e.g. [17].

B. Orders $\nu < 4$.

The structure of the effective Hamilton operator at leading order can be worked out straightforwardly applying the projection formalism as described in section II B to the lowest-order (i.e. with $\Delta_i = 0$) Hamilton density in Eq. (3.20). This leads to

$$V^{(0)} = \eta \left[H_{40}^2 - H_{21}^1 \frac{\lambda^1}{E_\pi} H_{21}^1 \right] \eta. \tag{3.21}$$

Here, the superscript of λ refers to the number of pions in the corresponding intermediate state, E_π is the total energy of n pions in the state λ^n , $E_\pi = \sum_{i=1}^n \omega_i$ where $\omega_i = \sqrt{\vec{q}_i^2 + M_\pi^2}$ is the energy of the pion with momentum \vec{q}_i . The subscripts a and b of H_{ab}^κ denote the number of nucleon and pion field operators, respectively. They are introduced in order to clarify the meaning of various terms in the effective potential. Clearly, the terms in Eq. (3.21) only give rise to one- and two-nucleon operators. The first corrections to the effective Hamiltonian arise at order $\nu = 2$. The relevant terms at this order read:

$$\begin{aligned}
V^{(2)} &= \eta \left[-H_{21}^1 \frac{\lambda^1}{E_\pi} H_{21}^1 \frac{\lambda^2}{E_\pi} H_{21}^1 \frac{\lambda^1}{E_\pi} H_{21}^1 + \frac{1}{2} H_{21}^1 \frac{\lambda^1}{E_\pi^2} H_{21}^1 \eta H_{21}^1 \frac{\lambda^1}{E_\pi} H_{21}^1 + \frac{1}{2} H_{21}^1 \frac{\lambda^1}{E_\pi} H_{21}^1 \eta H_{21}^1 \frac{\lambda^1}{E_\pi^2} H_{21}^1 \right. \\
&\quad \left. + H_{21}^1 \frac{\lambda^1}{E_\pi} H_{40}^2 \frac{\lambda^1}{E_\pi} H_{21}^1 - \frac{1}{2} H_{21}^1 \frac{\lambda^1}{E_\pi^2} H_{21}^1 \eta H_{40}^2 - \frac{1}{2} H_{40}^2 \eta H_{21}^1 \frac{\lambda^1}{E_\pi^2} H_{21}^1 \right] \eta.
\end{aligned} \tag{3.22}$$

Here we only list those terms which can generate four-nucleon operators. The complete list of terms at this order can be found in [12, 21]. The contribution to the 4NF from the operators in Eq. (3.22) can be represented schematically by disconnected diagrams shown in Fig. 1. It should be understood that diagrams in the method of unitary transformation have a different meaning compared to the ones arising in the context of time-ordered perturbation theory and serve merely to visualize the topology corresponding to a given sequence of operators H_{ab}^κ . We further emphasize that diagrams shown in this work represent the sum over all possible ‘‘time orderings’’ as depicted in Fig. 2.

The contributions to the 4NF from diagrams in Fig. 1 have been considered in Ref. [5] using time-ordered perturbation theory. In this approach, only the first and the fourth terms in Eq. (3.22) contribute to the effective Hamiltonian. Evaluating matrix elements of these terms corresponding to diagrams shown in Fig. 2 one obtains non-vanishing contributions to the 4NF. As pointed out in Ref. [5], the resulting 4NF cancels against the recoil corrections to the 2NF upon the iteration in the dynamical equation. The same sort of cancellation also takes place for the 3NF at $\nu = 2$ [5, 22].

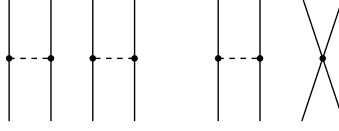


FIG. 1: Disconnected 4N diagrams at order $\nu = 2$. Solid and dashed lines represent nucleons and pions, respectively. Solid dots denote vertices with $\Delta_i = 0$ from Eq. (3.20).

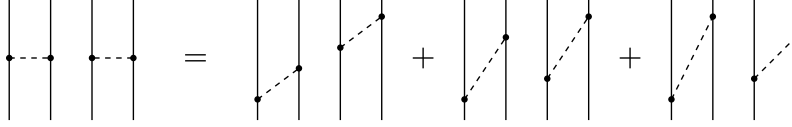


FIG. 2: Different “time orderings” for the first diagram in Fig. 1. respectively. Graphs resulting by the interchange of the nucleon lines are not shown.

In the method of unitary transformation, one has to take into account all terms in Eq. (3.22). It is easy to verify that the resulting 4NF vanishes due to an exact cancellation between the different terms in this equation. A similar cancellation occurs also for the 3NF [13, 23], see also [24], and for disconnected 2NF diagrams [21] at this chiral order. The corrections to the effective Hamilton operator at order $\nu = 3$ within the method of unitary transformation are discussed in detail in [13]. They give rise to at most tree-nucleon operators and will not be discussed in this work.

C. Order $\nu = 4$.

The first non-vanishing contributions to the 4NF arise at order $\nu = 4$. For the sake of a better overview, it is useful to divide the total contribution at this order into pieces with the same combinations of the coupling constants g_A and $C_{S,T}$. This leads to eight classes of terms which are discussed in detail below.

- **Class-I** contributions proportional to g_A^6 .

This class of contributions arises from all possible 4NF diagrams involving six vertices H_{21}^1 from the first line of Eq. (3.20). Using Eqs. (2.14)-(2.17) one obtains:

$$\begin{aligned}
 V^{(4)} = & \frac{1}{2} \eta \left[H_{21}^1 \frac{\lambda^1}{E_\pi} H_{21}^1 \eta H_{21}^1 \frac{\lambda^1}{E_\pi} H_{21}^1 \frac{\lambda^2}{E_\pi} H_{21}^1 \frac{\lambda^1}{E_\pi^2} H_{21}^1 + H_{21}^1 \frac{\lambda^1}{E_\pi} H_{21}^1 \eta H_{21}^1 \frac{\lambda^1}{E_\pi} H_{21}^1 \frac{\lambda^2}{E_\pi^2} H_{21}^1 \frac{\lambda^1}{E_\pi} H_{21}^1 \right. \\
 & + H_{21}^1 \frac{\lambda^1}{E_\pi} H_{21}^1 \eta H_{21}^1 \frac{\lambda^1}{E_\pi^2} H_{21}^1 \frac{\lambda^2}{E_\pi} H_{21}^1 \frac{\lambda^1}{E_\pi} H_{21}^1 + H_{21}^1 \frac{\lambda^1}{E_\pi^2} H_{21}^1 \eta H_{21}^1 \frac{\lambda^1}{E_\pi} H_{21}^1 \frac{\lambda^2}{E_\pi} H_{21}^1 \frac{\lambda^1}{E_\pi} H_{21}^1 \\
 & - H_{21}^1 \frac{\lambda^1}{E_\pi} H_{21}^1 \eta H_{21}^1 \frac{\lambda^1}{E_\pi} H_{21}^1 \eta H_{21}^1 \frac{\lambda^1}{E_\pi^3} H_{21}^1 - \frac{1}{4} H_{21}^1 \frac{\lambda^1}{E_\pi^2} H_{21}^1 \eta H_{21}^1 \frac{\lambda^1}{E_\pi} H_{21}^1 \eta H_{21}^1 \frac{\lambda^1}{E_\pi^2} H_{21}^1 \\
 & - \frac{3}{4} H_{21}^1 \frac{\lambda^1}{E_\pi} H_{21}^1 \eta H_{21}^1 \frac{\lambda^1}{E_\pi^2} H_{21}^1 \eta H_{21}^1 \frac{\lambda^1}{E_\pi^2} H_{21}^1 - H_{21}^1 \frac{\lambda^1}{E_\pi} H_{21}^1 \frac{\lambda^2}{E_\pi} H_{21}^1 \frac{\lambda^1}{E_\pi} H_{21}^1 \frac{\lambda^2}{E_\pi} H_{21}^1 \frac{\lambda^1}{E_\pi} H_{21}^1 \\
 & \left. - H_{21}^1 \frac{\lambda^1}{E_\pi} H_{21}^1 \frac{\lambda^2}{E_\pi} H_{21}^1 \frac{\lambda^3}{E_\pi} H_{21}^1 \frac{\lambda^2}{E_\pi} H_{21}^1 \frac{\lambda^1}{E_\pi} H_{21}^1 \right] \eta + \text{h.c.} . \tag{3.23}
 \end{aligned}$$

The corresponding contributions to the 4NF can, in principle, be evaluated straightforwardly by calculating matrix elements of the operators in Eq. (3.23) for all possible “time orderings” of diagrams shown in Fig. 3. Before giving the explicit results, it is important to address the issue whether the contribution $V^{(4)}$ is defined

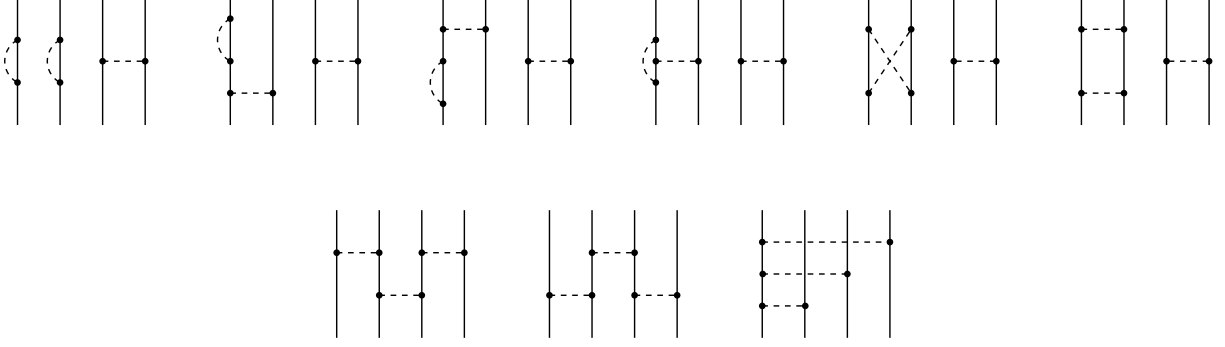


FIG. 3: Class-I contributions to the 4NF. For notation, see Figs. 1 and 2.

unambiguously. Generally, an effective Hamilton operator is defined modulo unitary transformations.² It should, therefore, be understood that terms in Eq. (3.23) correspond to *one* particular choice of the unitary transformation U . Indeed, Eq. (2.12) does not yield the most general parametrization of the operator U . The resulting effective Hamilton operator $\eta\tilde{H}\eta$ can be further modified via subsequent unitary transformations acting on the η -space. To be specific, consider the unitary transformation of the form:

$$U = e^S, \quad (3.24)$$

where S is an anti-hermitian operator acting on the η -space, $S \equiv \eta S \eta$, $S^\dagger = -S$. Further, let S be given by $S = \alpha_1 S_1 + \alpha_2 S_2$ with $\alpha_{1,2}$ being arbitrary real numbers and

$$\begin{aligned} S_1 &= \eta \left[H_{21}^1 \frac{\lambda^1}{E_\pi} H_{21}^1 \eta H_{21}^1 \frac{\lambda^1}{E_\pi^3} H_{21}^1 - H_{21}^1 \frac{\lambda^1}{E_\pi^3} H_{21}^1 \eta H_{21}^1 \frac{\lambda^1}{E_\pi} H_{21}^1 \right] \eta, \\ S_2 &= \eta \left[H_{21}^1 \frac{\lambda^1}{E_\pi} H_{21}^1 \frac{\lambda^2}{E_\pi} H_{21}^1 \frac{\lambda^1}{E_\pi^2} H_{21}^1 - H_{21}^1 \frac{\lambda^1}{E_\pi^2} H_{21}^1 \frac{\lambda^2}{E_\pi} H_{21}^1 \frac{\lambda^1}{E_\pi} H_{21}^1 \right] \eta. \end{aligned} \quad (3.25)$$

The operators S_1 and S_2 are the only possible ones that are invariant under the time-reversal operation and can be constructed out of four vertices H_{21}^1 provided the E_π 's are only allowed to appear in the denominators. Acting with the transformation U onto the lowest-order effective Hamilton operator,

$$H^{(0)} = \eta \left[H_{20}^2 + H_{40}^2 - H_{21}^1 \frac{\lambda^1}{E_\pi} H_{21}^1 \right] \eta, \quad (3.26)$$

where H_{20}^2 is the nonrelativistic kinetic energy term, the following additional terms in $V^{(4)}$ are generated:

$$\begin{aligned} \delta V^{(4)} &= [H^{(0)}, S] \\ &= -\alpha_1 \eta \left[H_{21}^1 \frac{\lambda^1}{E_\pi} H_{21}^1 \eta H_{21}^1 \frac{\lambda^1}{E_\pi} H_{21}^1 \frac{\lambda^1}{E_\pi^3} H_{21}^1 - H_{21}^1 \frac{\lambda^1}{E_\pi} H_{21}^1 \eta H_{21}^1 \frac{\lambda^1}{E_\pi^3} H_{21}^1 \eta H_{21}^1 \frac{\lambda^1}{E_\pi} H_{21}^1 \right] \eta \\ &\quad - \alpha_2 \eta \left[H_{21}^1 \frac{\lambda^1}{E_\pi} H_{21}^1 \eta H_{21}^1 \frac{\lambda^1}{E_\pi} H_{21}^1 \frac{\lambda^2}{E_\pi} H_{21}^1 \frac{\lambda^1}{E_\pi^2} H_{21}^1 - H_{21}^1 \frac{\lambda^1}{E_\pi} H_{21}^1 \eta H_{21}^1 \frac{\lambda^1}{E_\pi^2} H_{21}^1 \frac{\lambda^2}{E_\pi} H_{21}^1 \frac{\lambda^1}{E_\pi} H_{21}^1 \right] \eta \\ &\quad + \text{h.c.} + \dots \end{aligned} \quad (3.27)$$

Here, the ellipses refer to terms involving H_{20}^2 (H_{40}^2) which give rise to class-VIII (class-IV) corrections and will be considered below. The class-I contributions to the effective Hamiltonian, therefore, seem to be defined modulo the arbitrary constants α_1 and α_2 . We will now demonstrate that there exist one particular choice for

² Other sources of ambiguities related to field redefinitions in the Lagrangian and to the choice of the dynamical equation are discussed for one- and two-pion exchange potentials in Ref. [25].

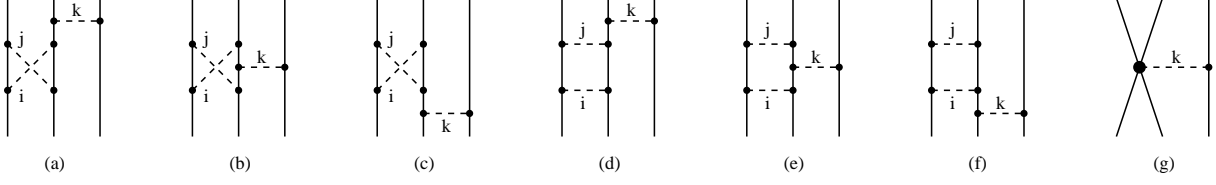


FIG. 4: Selected three-pion exchange contributions to the 3NF at order $\nu = 4$ (graphs (a)-(f)) and one-pion exchange 3NF at order $\nu = 4$. Filled circle denotes the leading $\pi N N N N$ vertex with $\Delta_i = 1$. For remaining notation, see Figs. 1 and 2.

these constants which is strongly preferable. To that aim consider *three-nucleon* forces generated by terms in Eqs. (3.23), (3.27) and involving one-pion exchange between two nucleons, see Fig. 4, diagrams (a)-(f). We can generally express the structure of the 3NF in the form

$$V_{3N}^i = M_{3N}^i \bar{V}_{3N}^i. \quad (3.28)$$

Here, M_{3N}^i represents the spin, isospin and momentum structure which results from vertices entering a diagram i and \bar{V}_{3N}^i denotes the corresponding energy denominators. Evaluating matrix elements of operators in Eqs. (3.23) and (3.27) for all possible “time orderings” of diagrams (a)-(f) in Fig. 4 yields

$$\begin{aligned} \bar{V}_{3N}^a &= \frac{4}{\omega_i^3 \omega_j \omega_k}, \\ \bar{V}_{3N}^b &= -\frac{4}{\omega_i^3 \omega_j \omega_k} - \frac{4}{\omega_i \omega_j^3 \omega_k}, \\ \bar{V}_{3N}^c &= \bar{V}_{3N}^a \Big|_{\{a,i,j\} \rightarrow \{c,j,i\}}, \\ \bar{V}_{3N}^d &= -4 \frac{1-2\alpha_2}{\omega_i \omega_j \omega_k^3} + \frac{1+2\alpha_1}{\omega_i \omega_j^2 \omega_k^2} + 2 \frac{1+2\alpha_1}{\omega_i \omega_j^3 (\omega_j + \omega_k)} \\ &\quad + \frac{1}{\omega_k} \left(-4 \frac{1-2\alpha_2}{\omega_i^3 \omega_j} + 2 \frac{1-2\alpha_1 - 8\alpha_2}{\omega_i \omega_j^3} - \frac{1+2\alpha_1}{\omega_i \omega_j^2 (\omega_i + \omega_j)} + \frac{1+2\alpha_1}{\omega_i^2 \omega_j (\omega_i + \omega_j)} \right), \\ \bar{V}_{3N}^e &= 8 \frac{1-2\alpha_2}{\omega_i \omega_j \omega_k^3} - \frac{1+2\alpha_1}{\omega_i \omega_j^2 \omega_k^2} - \frac{1+2\alpha_1}{\omega_i^2 \omega_j \omega_k^2} - 2 \frac{1+2\alpha_1}{\omega_i \omega_j^3 (\omega_j + \omega_k)} - 2 \frac{1+2\alpha_1}{\omega_i^3 \omega_j (\omega_i + \omega_k)} \\ &\quad + \frac{1}{\omega_k} \left(2 \frac{1+2\alpha_1 + 4\alpha_2}{\omega_i \omega_j^3} + 2 \frac{1+2\alpha_1 + 4\alpha_2}{\omega_i^3 \omega_j} \right), \\ \bar{V}_{3N}^f &= \bar{V}_{3N}^d \Big|_{\{d,i,j\} \rightarrow \{f,j,i\}}. \end{aligned} \quad (3.29)$$

The contributions from crossed-box diagrams (a-c) exhibit the expected dependence on the pion energy ω_k which leads to the usual static one-pion exchange potential (OPEP) $\propto \omega_k^{-2} = 1/(\vec{q}_k^2 + M_\pi^2)$. The additional factor of ω_k^{-1} results from the pion phase-space factors. Notice further that $V_{3N}^{a,b,c}$ do not depend on the parameters $\alpha_{1,2}$ ³. The contributions from the box diagrams (d-f) do, however, depend on $\alpha_{1,2}$ and involve terms that cannot be associated with the static OPEP between the second and the third nucleons. For example, terms proportional to ω_k^{-2} in the last three lines of Eq. (3.29) lead to the 3N potential proportional to $(\vec{q}_k^2 + M_\pi^2)^{-3/2}$ which has a cut starting at $\vec{q}^2 = -M_\pi^2$. The presence of such a cut which is not produced by multi-particle intermediate states appears, at first sight, rather puzzling. One should, however, keep in mind that we are dealing here with the non-iterative part of the scattering amplitude which gives rise to nuclear forces. Its analytic structure needs, in principle, not to coincide with the one of the full amplitude. A more serious problem due to the appearance of the “unphysical” terms in Eq. (3.29) is non-renormalizability of the corresponding 3NF. Indeed, one can easily verify using dimensional arguments that the loop integrals entering, for example, the ω_k^{-3} (ω_k^{-2}) terms give rise

³ The independence on α_1 follows directly from Eq. (3.27).

to cubic and linear (quadratic and logarithmic) ultraviolet divergences. The only relevant counter term which is available at this order and which can be used to absorb the infinities is H_{41}^4 with one pion and four nucleon field operators. It is proportional to the LEC D and enters the 3NF at order $\nu = 3$, see diagram (g) in Fig. 4, which arises from

$$V^{(3)} = -\eta \left[H_{41}^4 \frac{\lambda^1}{\omega_k} H_{21}^1 + H_{21}^1 \frac{\lambda^1}{\omega_k} H_{41}^4 \right] \eta, \quad (3.30)$$

and leads to $\bar{V}_{3N}^g = -2/\omega_k$ [5, 6]. The contributions to the 3NF in Eq. (3.29) with a different dependence on ω_k can, obviously, not be renormalized in this way. Again, it should be understood that the above mentioned difficulty does not affect S-matrix elements. All ‘‘problematic’’ divergences that enter the 3NF have to cancel against the divergences arising from iterative contributions to the amplitude in such a way that the resulting S-matrix is renormalizable in the usual sense. For the purpose of describing the few-nucleon dynamics based on the Schrödinger equation, it is, however, desirable to have a well-defined effective Hamilton operator. The difficulty with the non-renormalizability of the 3NF in Eq. (3.29) can be avoided if one requires that only the ω_k^{-1} terms are present, i.e. the OPEP factorizes out in diagrams (d-f) in Fig. 4. This can be achieved via a suitable choice of the η -space unitary transformation by setting

$$\alpha_1 = -\alpha_2 = -\frac{1}{2}. \quad (3.31)$$

This choice leads to the following remarkably simple expressions:

$$\begin{aligned} \bar{V}_{3N}^d &= -\frac{4}{\omega_i \omega_j^3 \omega_k}, \\ \bar{V}_{3N}^e &= \frac{4}{\omega_i^3 \omega_j \omega_k} + \frac{4}{\omega_i \omega_j^3 \omega_k}, \\ \bar{V}_{3N}^f &= V_{3N}^d \Big|_{\{d,i,j\} \rightarrow \{f,j,i\}}. \end{aligned} \quad (3.32)$$

These considerations may remind one of the recent findings in the context of large- N_c QCD [26, 27, 28]. There it was found that the multiple-meson exchange potential derived in the energy-dependent formulation is inconsistent with large- N_c counting rules. The consistency could be maintained using a different (but completely equivalent) form of the potential based on the energy-independent formalism, see Ref. [28] for more details.

Choosing the parameters $\alpha_{1,2}$ as described above, it is a straightforward exercise to calculate the contributions to the 4NF associated with the diagrams in Fig. 3. We found that all disconnected graphs lead to vanishing contributions regardless of the values of $\alpha_{1,2}$. From the connected diagrams in the second row in Fig. 3, only the first two generate non-vanishing contributions to the 4NF which take the form:

$$\begin{aligned} V_{\text{Class-I}} &= -\frac{2g_A^6}{(2F_\pi)^6} \frac{\vec{\sigma}_1 \cdot \vec{q}_1 \vec{\sigma}_4 \cdot \vec{q}_4}{[\vec{q}_1^2 + M_\pi^2] [\vec{q}_{12}^2 + M_\pi^2]^2 [\vec{q}_4^2 + M_\pi^2]} \\ &\times \left[(\boldsymbol{\tau}_1 \cdot \boldsymbol{\tau}_4 \boldsymbol{\tau}_2 \cdot \boldsymbol{\tau}_3 - \boldsymbol{\tau}_1 \cdot \boldsymbol{\tau}_3 \boldsymbol{\tau}_2 \cdot \boldsymbol{\tau}_4) \vec{q}_1 \cdot \vec{q}_{12} \vec{q}_4 \cdot \vec{q}_{12} + \boldsymbol{\tau}_1 \times \boldsymbol{\tau}_2 \cdot \boldsymbol{\tau}_4 \vec{q}_1 \cdot \vec{q}_{12} \vec{q}_{12} \times \vec{q}_4 \cdot \vec{\sigma}_3 \right. \\ &\left. + \boldsymbol{\tau}_1 \times \boldsymbol{\tau}_3 \cdot \boldsymbol{\tau}_4 \vec{q}_4 \cdot \vec{q}_{12} \vec{q}_1 \times \vec{q}_{12} \cdot \vec{\sigma}_2 + \boldsymbol{\tau}_1 \cdot \boldsymbol{\tau}_4 \vec{q}_{12} \times \vec{q}_1 \cdot \vec{\sigma}_2 \vec{q}_{12} \times \vec{q}_4 \cdot \vec{\sigma}_3 \right] + \text{all perm..} \end{aligned} \quad (3.33)$$

Here, the subscripts refer to the nucleon labels and $\vec{q}_i = \vec{p}_i' - \vec{p}_i$ with \vec{p}_i' and \vec{p}_i being the final and initial momenta of the nucleon i . Further, $\vec{q}_{12} = \vec{q}_1 + \vec{q}_2 = -\vec{q}_3 - \vec{q}_4 = -\vec{q}_{34}$ is the momentum transfer between the nucleon pairs 12 and 34. We have verified that the obtained expression for the class-I 4NF remains unchanged if one considers a larger class of unitary transformations in Eq. (3.24) with the operator S involving terms with pion energies in the numerators. Although the renormalizability condition does not completely fix the corresponding η -space unitary transformations in that case, the remaining ambiguity does not affect nuclear forces at the considered order. Notice further that the contribution from the last graph in Fig. 3 only vanishes if the constants $\alpha_{1,2}$ are chosen according to Eq. (3.31). Finally, it should be emphasized that the ambiguity due to the additional η -space unitary transformations does not show up at lower orders in the chiral expansion since it is not possible to construct non-vanishing anti-hermitian operators S with just two vertices H_{21}^1 .

- **Class-II** contributions proportional to g_A^4 .

These contributions arise from 4N diagrams involving four vertices H_{21}^1 and one insertion of the Weinberg-Tomozawa vertex H_{22}^2 , see Fig. 5. In addition, there are diagrams with one insertion of the nonlinear pion

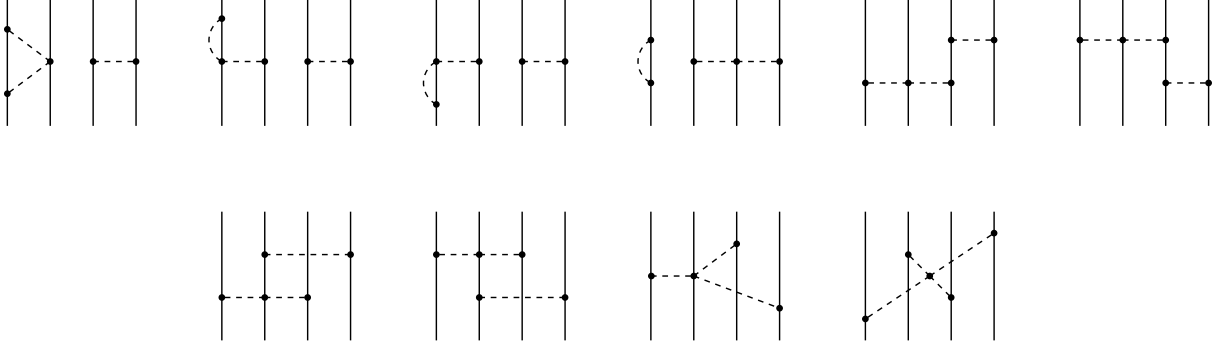


FIG. 5: Class-II contributions to the 4NF. For notation, see Figs. 1 and 2.

and pion-nucleon interactions H_{04} and H_{23} , respectively. Using Eqs. (2.14)-(2.17) one obtains the following contributions to the class-II effective Hamilton operator:

$$\begin{aligned}
V^{(4)} = & \eta \left[-\frac{1}{2} H_{21}^1 \frac{\lambda^1}{E_\pi} H_{21}^1 \eta H_{21}^1 \frac{\lambda^1}{E_\pi} H_{21}^1 \frac{\lambda^2}{E_\pi^2} H_{22}^2 - \frac{1}{2} H_{21}^1 \frac{\lambda^1}{E_\pi} H_{21}^1 \eta H_{21}^1 \frac{\lambda^1}{E_\pi} H_{22}^2 \frac{\lambda^1}{E_\pi^2} H_{21}^1 \right. \\
& - \frac{1}{2} H_{21}^1 \frac{\lambda^1}{E_\pi} H_{21}^1 \eta H_{22}^2 \frac{\lambda^2}{E_\pi} H_{21}^1 \frac{\lambda^1}{E_\pi^2} H_{21}^1 - \frac{1}{2} H_{21}^1 \frac{\lambda^1}{E_\pi} H_{21}^1 \eta H_{21}^1 \frac{\lambda^1}{E_\pi^2} H_{21}^1 \frac{\lambda^2}{E_\pi} H_{22}^2 \\
& - \frac{1}{2} H_{21}^1 \frac{\lambda^1}{E_\pi} H_{21}^1 \eta H_{21}^1 \frac{\lambda^1}{E_\pi^2} H_{22}^2 \frac{\lambda^1}{E_\pi} H_{21}^1 - \frac{1}{2} H_{21}^1 \frac{\lambda^1}{E_\pi} H_{21}^1 \eta H_{22}^2 \frac{\lambda^2}{E_\pi^2} H_{21}^1 \frac{\lambda^1}{E_\pi} H_{21}^1 \\
& - \frac{1}{2} H_{21}^1 \frac{\lambda^1}{E_\pi^2} H_{21}^1 \eta H_{21}^1 \frac{\lambda^1}{E_\pi} H_{21}^1 \frac{\lambda^2}{E_\pi} H_{22}^2 - \frac{1}{2} H_{21}^1 \frac{\lambda^1}{E_\pi^2} H_{21}^1 \eta H_{21}^1 \frac{\lambda^1}{E_\pi} H_{22}^2 \frac{\lambda^1}{E_\pi} H_{21}^1 \\
& - \frac{1}{2} H_{21}^1 \frac{\lambda^1}{E_\pi^2} H_{21}^1 \eta H_{22}^2 \frac{\lambda^2}{E_\pi} H_{21}^1 \frac{\lambda^1}{E_\pi} H_{21}^1 + \frac{1}{2} H_{21}^1 \frac{\lambda^1}{E_\pi} H_{21}^1 \frac{\lambda^2}{E_\pi} H_{22}^2 \frac{\lambda^2}{E_\pi} H_{21}^1 \frac{\lambda^1}{E_\pi} H_{21}^1 \\
& + H_{21}^1 \frac{\lambda^1}{E_\pi} H_{21}^1 \frac{\lambda^2}{E_\pi} H_{21}^1 \frac{\lambda^1}{E_\pi} H_{21}^1 \frac{\lambda^2}{E_\pi} H_{22}^2 + H_{21}^1 \frac{\lambda^1}{E_\pi} H_{21}^1 \frac{\lambda^2}{E_\pi} H_{21}^1 \frac{\lambda^1}{E_\pi} H_{22}^2 \frac{\lambda^1}{E_\pi} H_{21}^1 \\
& + H_{21}^1 \frac{\lambda^1}{E_\pi} H_{21}^1 \frac{\lambda^2}{E_\pi} H_{21}^1 \frac{\lambda^3}{E_\pi} H_{21}^1 \frac{\lambda^2}{E_\pi} H_{22}^2 + H_{21}^1 \frac{\lambda^1}{E_\pi} H_{21}^1 \frac{\lambda^2}{E_\pi} H_{21}^1 \frac{\lambda^3}{E_\pi} H_{22}^2 \frac{\lambda^1}{E_\pi} H_{21}^1 \\
& - H_{21}^1 \frac{\lambda^1}{E_\pi} H_{21}^1 \frac{\lambda^2}{E_\pi} H_{21}^1 \frac{\lambda^3}{E_\pi} H_{23}^3 - H_{21}^1 \frac{\lambda^1}{E_\pi} H_{21}^1 \frac{\lambda^2}{E_\pi} H_{23}^3 \frac{\lambda^1}{E_\pi} H_{21}^1 \\
& + H_{21}^1 \frac{\lambda^1}{E_\pi} H_{21}^1 \frac{\lambda^2}{E_\pi} H_{21}^1 \frac{\lambda^3}{E_\pi} H_{21}^1 \frac{\lambda^4}{E_\pi} H_{04}^4 + H_{21}^1 \frac{\lambda^1}{E_\pi} H_{21}^1 \frac{\lambda^2}{E_\pi} H_{21}^1 \frac{\lambda^3}{E_\pi} H_{04}^4 \frac{\lambda^1}{E_\pi} H_{21}^1 \\
& \left. + \frac{1}{2} H_{21}^1 \frac{\lambda^1}{E_\pi} H_{21}^1 \frac{\lambda^2}{E_\pi} H_{04}^4 \frac{\lambda^2}{E_\pi} H_{21}^1 \frac{\lambda^1}{E_\pi} H_{21}^1 \right] \eta + \text{h.c.} . \tag{3.34}
\end{aligned}$$

Similar to the previously considered class-I contributions, we employ additional η -space unitary transformations with the operator S in Eq. (3.24) given by $S = \alpha_3 S_3 + \alpha_4 S_4 + \alpha_5 S_5$ where α_i are real constants and

$$\begin{aligned}
S_3 &= \eta \left[H_{21}^1 \frac{\lambda^1}{E_\pi^2} H_{22}^2 \frac{\lambda^1}{E_\pi} H_{21}^1 - H_{21}^1 \frac{\lambda^1}{E_\pi} H_{22}^2 \frac{\lambda^1}{E_\pi^2} H_{21}^1 \right] \eta, \\
S_4 &= \eta \left[H_{22}^2 \frac{\lambda^2}{E_\pi^2} H_{21}^1 \frac{\lambda^1}{E_\pi} H_{21}^1 - H_{21}^1 \frac{\lambda^1}{E_\pi} H_{21}^1 \frac{\lambda^2}{E_\pi^2} H_{22}^2 \right] \eta, \\
S_5 &= \eta \left[H_{22}^2 \frac{\lambda^2}{E_\pi} H_{21}^1 \frac{\lambda^1}{E_\pi^2} H_{21}^1 - H_{21}^1 \frac{\lambda^1}{E_\pi^2} H_{21}^1 \frac{\lambda^2}{E_\pi} H_{22}^2 \right] \eta. \tag{3.35}
\end{aligned}$$

The operators S_3 , S_4 and S_5 are the only time-reversal invariant anti-hermitian operators that can be constructed out of two vertices H_{21}^1 and one Weinberg-Tomozawa vertex H_{22}^2 with E_π 's appearing only in the denominators.

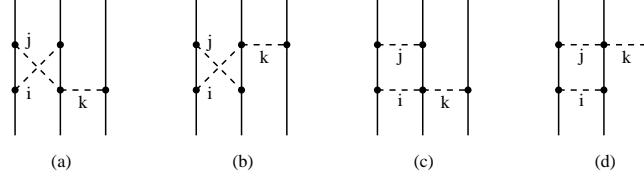


FIG. 6: Class-II three-nucleon diagrams which provide constraints on α_3 , α_4 and α_5 as explained in the text. For notation, see Figs. 1 and 2.

The corresponding α_i -dependent class-II contributions to the effective Hamilton operator read:

$$\begin{aligned}
\delta V^{(4)} &= [H^{(0)}, S] \\
&= -\alpha_3 \eta \left[H_{21}^1 \frac{\lambda^1}{E_\pi} H_{21}^1 \eta H_{21}^1 \frac{\lambda^1}{E_\pi^2} H_{22}^2 \frac{\lambda^1}{E_\pi} H_{21}^1 - H_{21}^1 \frac{\lambda^1}{E_\pi} H_{21}^1 \eta H_{21}^1 \frac{\lambda^1}{E_\pi} H_{22}^2 \frac{\lambda^1}{E_\pi^2} H_{21}^1 \right] \eta \\
&\quad - \alpha_4 \eta \left[H_{21}^1 \frac{\lambda^1}{E_\pi} H_{21}^1 \eta H_{22}^2 \frac{\lambda^2}{E_\pi^2} H_{21}^1 \frac{\lambda^1}{E_\pi} H_{21}^1 - H_{21}^1 \frac{\lambda^1}{E_\pi} H_{21}^1 \eta H_{21}^1 \frac{\lambda^1}{E_\pi} H_{21}^1 \frac{\lambda^2}{E_\pi^2} H_{22}^2 \right] \eta \\
&\quad - \alpha_5 \eta \left[H_{21}^1 \frac{\lambda^1}{E_\pi} H_{21}^1 \eta H_{22}^2 \frac{\lambda^2}{E_\pi} H_{21}^1 \frac{\lambda^1}{E_\pi^2} H_{21}^1 - H_{21}^1 \frac{\lambda^1}{E_\pi} H_{21}^1 \eta H_{21}^1 \frac{\lambda^1}{E_\pi^2} H_{21}^1 \frac{\lambda^2}{E_\pi} H_{22}^2 \right] \eta + \text{h.c.} + \dots,
\end{aligned} \tag{3.36}$$

where the ellipses refer to terms involving an insertion of either the nucleon kinetic energy H_{20}^2 or the contact interaction H_{40}^2 (class-V contributions). The constants α_3 , α_4 and α_5 are constrained by the requirement that the OPEP factorizes out in the 3NF diagrams shown in Fig. 6. This guarantees that all ultraviolet divergences arising in the corresponding loop integrals are absorbable into a redefinition of the LEC D entering the 3NF (g) in Fig. 4. We emphasize that the 3NF diagrams shown in Fig. 6 are not the only possible class-II diagrams with a single pion being exchanged between the first two and the third nucleons. All other 3NF contributions which are not shown in Fig. 6 are found to be proportional to ω_k^{-1} irrespectively on the values of α_i and, therefore, do not constrain these constants. Evaluating matrix elements of the operators in Eqs. (3.34) and (3.36) for all possible ‘‘time orderings’’ of diagrams in Fig. 6 yields:

$$\begin{aligned}
\bar{V}_{3N}^a &= \frac{4}{\omega_i \omega_j \omega_k}, \\
\bar{V}_{3N}^b &= -\bar{V}_{3N}^a \Big|_{\{a,i,j\} \rightarrow \{b,j,i\}}, \\
\bar{V}_{3N}^c &= 4 \frac{\alpha_3 + \alpha_5}{\omega_j \omega_k^2} + 4 \frac{1 - 2\alpha_4 + 4\alpha_5}{\omega_i \omega_j (\omega_i + \omega_k)} - 2 \frac{3 - 2\alpha_4 + 4\alpha_5}{\omega_i \omega_j \omega_k} - 4 \frac{\alpha_3 + \alpha_5}{\omega_i^2 \omega_j}, \\
\bar{V}_{3N}^d &= -\bar{V}_{3N}^c \Big|_{\{c,i,j\} \rightarrow \{d,j,i\}}.
\end{aligned} \tag{3.37}$$

In order to simplify the above expressions, we have taken into account the pion kinetic energy arising from the time derivative in the Weinberg-Tomozawa vertex according to:

$$\begin{aligned}
\langle \pi_a(\vec{q}_1) N | H_{22}^2 | \pi_b(\vec{q}_2) N \rangle &= -(\omega_{\vec{q}_1} + \omega_{\vec{q}_2}) v_{ab}, \\
\langle \pi_a(\vec{q}_1) \pi_b(\vec{q}_2) N | H_{22}^2 | N \rangle &= -(\omega_{\vec{q}_1} - \omega_{\vec{q}_2}) v_{ab}, \\
\langle N | H_{22}^2 | \pi_a(\vec{q}_1) \pi_b(\vec{q}_2) N \rangle &= (\omega_{\vec{q}_1} - \omega_{\vec{q}_2}) v_{ab}.
\end{aligned} \tag{3.38}$$

Here a and b are the pion isospin quantum numbers and

$$v_{ab} = \frac{i}{8F_\pi^2} \epsilon_{abc} \tau_c \frac{1}{\sqrt{\omega_{\vec{q}_1} \omega_{\vec{q}_2}}}. \tag{3.39}$$

The OPEP between the pair of the first two and the third nucleon factorizes out in Eq. (3.37) if the constants α_i fulfill the relations

$$\alpha_3 = -\alpha_5, \quad \alpha_4 = \frac{1}{2} + 2\alpha_5. \tag{3.40}$$

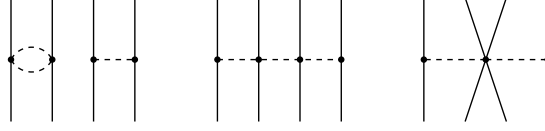


FIG. 7: Class-III contributions to the 4NF. For notation, see Figs. 1 and 2.

With this choice, the expressions for \bar{V}_{3N}^c and \bar{V}_{3N}^d from box diagrams take a particularly simple form and are identical to the ones arising from the cross-box contributions \bar{V}_{3N}^a and \bar{V}_{3N}^b . We further emphasize that although these constraints do not completely fix the corresponding unitary transformations, the results for all class-II 3NFs and 4NFs turn out to be independent on α_i . We found that the disconnected diagrams in Fig. 5 do not yield 4NFs irrespective of the values of α_i . Choosing α_i as specified in Eq. (3.40), the last two diagrams in the first row in Fig. 5 lead to vanishing 4NFs while the contribution from the first two diagrams in the second row is given by

$$V_{\text{Class-II}} = \frac{2g_A^4}{(2F_\pi)^6} \frac{\vec{\sigma}_1 \cdot \vec{q}_1 \vec{\sigma}_4 \cdot \vec{q}_4}{[\vec{q}_1^2 + M_\pi^2][\vec{q}_{12}^2 + M_\pi^2][\vec{q}_4^2 + M_\pi^2]} \left[(\boldsymbol{\tau}_1 \cdot \boldsymbol{\tau}_4 \boldsymbol{\tau}_2 \cdot \boldsymbol{\tau}_3 - \boldsymbol{\tau}_1 \cdot \boldsymbol{\tau}_3 \boldsymbol{\tau}_2 \cdot \boldsymbol{\tau}_4) \vec{q}_{12} \cdot \vec{q}_4 \right. \\ \left. + \boldsymbol{\tau}_1 \times \boldsymbol{\tau}_2 \cdot \boldsymbol{\tau}_4 \vec{q}_{12} \times \vec{q}_4 \cdot \vec{\sigma}_3 \right] + \text{all perm.} . \quad (3.41)$$

The last two diagrams in the second row of Fig. 5 do not involve reducible topologies. The corresponding 4NFs can, therefore, be evaluated using the Feynman graph technique with no need to consider all possible “time-ordered” diagrams. Using the Feynman rule

$$\frac{g_A}{4F_\pi^3} [\tau^a \delta^{bc} \vec{\sigma} \cdot (4\alpha \vec{q}_1 + (4\alpha - 1)(\vec{q}_2 + \vec{q}_3)) + 2 \text{ cycl. perm.}] , \quad (3.42)$$

for the $\pi\pi\pi NN$ vertex and

$$\frac{i}{F_\pi^2} [\delta^{ab} \delta^{cd} ((q_1 + q_2)^2 - M_\pi^2) + 2\alpha [4M_\pi^2 - q_1^2 - q_2^2 - q_3^2 - q_4^2]) + 2 \text{ cycl. perm.}] , \quad (3.43)$$

for the $\pi\pi\pi\pi$ -vertex, where the superscripts refer to the pion isospin quantum numbers and q_i denote the corresponding pion outgoing momenta, we obtain the following result:

$$V_{\text{Class-II}} = \frac{g_A^4}{(2F_\pi)^6} \frac{\vec{\sigma}_2 \cdot \vec{q}_2 \vec{\sigma}_3 \cdot \vec{q}_3 \vec{\sigma}_4 \cdot \vec{q}_4}{[\vec{q}_2^2 + M_\pi^2][\vec{q}_3^2 + M_\pi^2][\vec{q}_4^2 + M_\pi^2]} \boldsymbol{\tau}_1 \cdot \boldsymbol{\tau}_2 \boldsymbol{\tau}_3 \cdot \boldsymbol{\tau}_4 \left[\vec{\sigma}_1 \cdot (\vec{q}_3 + \vec{q}_4) - 4\alpha \vec{\sigma}_1 \cdot (\vec{q}_2 + \vec{q}_3 + \vec{q}_4) \right] \\ + \frac{g_A^4}{2(2F_\pi)^6} \frac{\vec{\sigma}_1 \cdot \vec{q}_1 \vec{\sigma}_2 \cdot \vec{q}_2 \vec{\sigma}_3 \cdot \vec{q}_3 \vec{\sigma}_4 \cdot \vec{q}_4}{[\vec{q}_1^2 + M_\pi^2][\vec{q}_2^2 + M_\pi^2][\vec{q}_3^2 + M_\pi^2][\vec{q}_4^2 + M_\pi^2]} \boldsymbol{\tau}_1 \cdot \boldsymbol{\tau}_2 \boldsymbol{\tau}_3 \cdot \boldsymbol{\tau}_4 \left[(\vec{q}_1 + \vec{q}_2)^2 + M_\pi^2 \right. \\ \left. - 2\alpha (4M_\pi^2 + \vec{q}_1^2 + \vec{q}_2^2 + \vec{q}_3^2 + \vec{q}_4^2) \right] + \text{all perm.} . \quad (3.44)$$

It is easy to see that terms proportional to α cancel out each other. Thus, while the individual contributions from the last two diagrams in Fig. 5 do depend on the arbitrary constant α , the α -dependence drops out completely in the total result. Notice further that the individual contributions of these two diagrams are given in Ref. [11] for the choice $\alpha = 0$.

- **Class-III** contributions proportional to g_A^2 .

This class of contributions arises from diagrams with two insertions of the Weinberg-Tomozawa vertex H_{22}^2 or one insertion of the $\pi\pi NNNN$ vertex H_{42}^4 defined in the last line of Eq. (3.20), see Fig. 7. The corresponding operators read:

$$V^{(4)} = \eta \left[\frac{1}{2} H_{21}^1 \frac{\lambda^1}{E_\pi} H_{21}^1 \eta H_{22}^2 \frac{\lambda^2}{E_\pi} H_{22}^2 + \frac{1}{2} H_{21}^1 \frac{\lambda^1}{E_\pi} H_{21}^1 \eta H_{22}^2 \frac{\lambda^2}{E_\pi} H_{22}^2 - H_{21}^1 \frac{\lambda^1}{E_\pi} H_{21}^1 \frac{\lambda^2}{E_\pi} H_{22}^2 \frac{\lambda^2}{E_\pi} H_{22}^2 \right. \\ \left. - H_{21}^1 \frac{\lambda^1}{E_\pi} H_{22}^2 \frac{\lambda^1}{E_\pi} H_{21}^1 \frac{\lambda^2}{E_\pi} H_{22}^2 - \frac{1}{2} H_{21}^1 \frac{\lambda^1}{E_\pi} H_{22}^2 \frac{\lambda^1}{E_\pi} H_{22}^2 \frac{\lambda^1}{E_\pi} H_{21}^1 - H_{21}^1 \frac{\lambda^1}{E_\pi} H_{22}^2 \frac{\lambda^3}{E_\pi} H_{21}^1 \frac{\lambda^2}{E_\pi} H_{22}^2 \right]$$

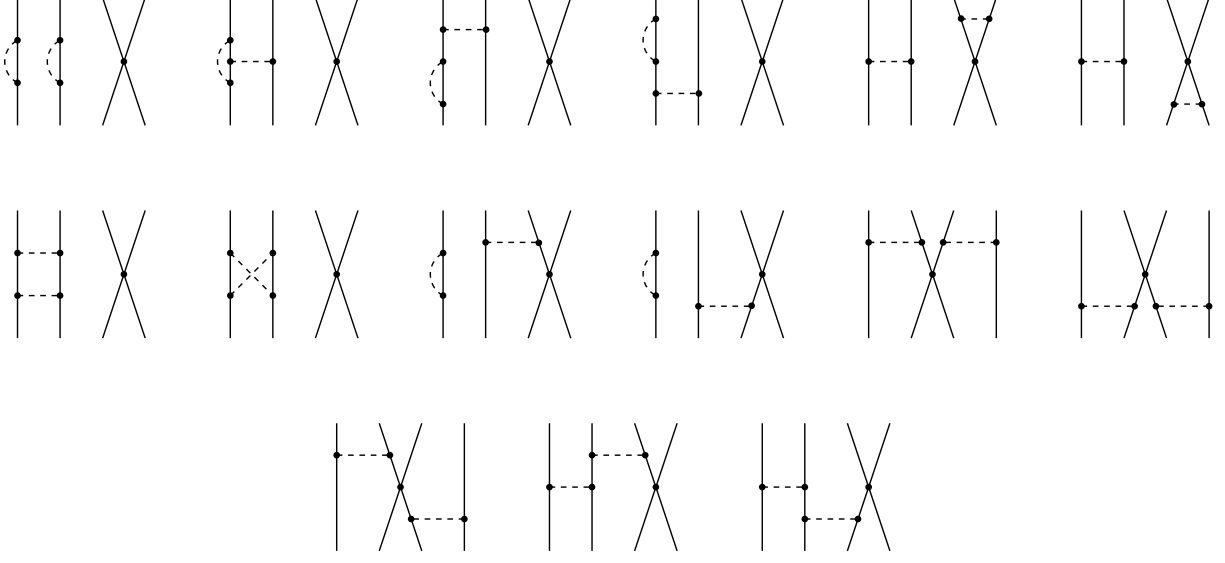


FIG. 8: Class-IV contributions to the 4NF. For notation, see Figs. 1 and 2.

$$\begin{aligned}
& -\frac{1}{2}H_{21}^1 \frac{\lambda^1}{E_\pi} H_{22}^2 \frac{\lambda^3}{E_\pi} H_{22}^2 \frac{\lambda^1}{E_\pi} H_{21}^1 - \frac{1}{2}H_{22}^2 \frac{\lambda^2}{E_\pi} H_{21}^1 \frac{\lambda^3}{E_\pi} H_{21}^1 \frac{\lambda^2}{E_\pi} H_{22}^2 - \frac{1}{2}H_{22}^2 \frac{\lambda^2}{E_\pi} H_{21}^1 \frac{\lambda^1}{E_\pi} H_{21}^1 \frac{\lambda^2}{E_\pi} H_{22}^2 \\
& + H_{21}^1 \frac{\lambda^1}{E_\pi} H_{21}^1 \frac{\lambda^2}{E_\pi} H_{42}^4 + \frac{1}{2}H_{21}^1 \frac{\lambda^1}{E_\pi} H_{42}^4 \frac{\lambda^1}{E_\pi} H_{21}^1 \Big] \eta + \text{h.c.} . \tag{3.45}
\end{aligned}$$

The class-III contributions are not affected by the η -space unitary transformations. The disconnected diagram is again found to produce vanishing 4NF contribution. The 4NF contributions from the last two diagrams derived using Eq. (3.45) do not vanish individually but cancel each other. This result can also be obtained in a simpler way using the Feynman graph technique. In this framework, one only has to consider the second graph in Fig. 7. The last diagram does not appear since there is no $\pi\pi NNNN$ vertex of dimension $\Delta_i = 0$ in the Lagrangian. Due to the four-momentum conservation at each vertex and the fact that the Weinberg-Tomozawa vertex contains a time derivative of the pion field, the contribution of the second Feynman diagram in Fig. 7 is suppressed by Q^2/m^2 and, therefore, shifted to higher orders.

- **Class-IV** contributions proportional to $g_A^4 C_{S,T}$.

This class of contributions arises from diagrams involving four vertices H_{21}^1 and one insertion of the leading-order contact interactions H_{40}^2 , see Fig. 8. From Eqs. (2.14)-(2.17), one obtains:

$$\begin{aligned}
V^{(4)} = & \eta \left[-\frac{1}{2}H_{21}^1 \frac{\lambda^1}{E_\pi} H_{21}^1 \eta H_{21}^1 \frac{\lambda^1}{E_\pi} H_{40}^2 \frac{\lambda^1}{E_\pi^2} H_{21}^1 - \frac{1}{2}H_{21}^1 \frac{\lambda^1}{E_\pi} H_{21}^1 \eta H_{21}^1 \frac{\lambda^1}{E_\pi^2} H_{40}^2 \frac{\lambda^1}{E_\pi} H_{21}^1 \right. \\
& - \frac{1}{2}H_{21}^1 \frac{\lambda^1}{E_\pi^2} H_{21}^1 \eta H_{21}^1 \frac{\lambda^1}{E_\pi} H_{40}^2 \frac{\lambda^1}{E_\pi} H_{21}^1 - \frac{1}{2}H_{40}^2 \eta H_{21}^1 \frac{\lambda^1}{E_\pi} H_{21}^1 \frac{\lambda^2}{E_\pi} H_{21}^1 \frac{\lambda^1}{E_\pi^2} H_{21}^1 \\
& - \frac{1}{2}H_{40}^2 \eta H_{21}^1 \frac{\lambda^1}{E_\pi} H_{21}^1 \frac{\lambda^2}{E_\pi^2} H_{21}^1 \frac{\lambda^1}{E_\pi} H_{21}^1 - \frac{1}{2}H_{40}^2 \eta H_{21}^1 \frac{\lambda^1}{E_\pi^2} H_{21}^1 \frac{\lambda^2}{E_\pi} H_{21}^1 \frac{\lambda^1}{E_\pi} H_{21}^1 \\
& + \frac{1}{2}H_{40}^2 \eta H_{21}^1 \frac{\lambda^1}{E_\pi} H_{21}^1 \eta H_{21}^1 \frac{\lambda^1}{E_\pi^3} H_{21}^1 + \frac{3}{8}H_{40}^2 \eta H_{21}^1 \frac{\lambda^1}{E_\pi^2} H_{21}^1 \eta H_{21}^1 \frac{\lambda^1}{E_\pi^2} H_{21}^1 \\
& + \frac{1}{2}H_{21}^1 \frac{\lambda^1}{E_\pi} H_{21}^1 \eta H_{40}^2 \eta H_{21}^1 \frac{\lambda^1}{E_\pi^3} H_{21}^1 + \frac{1}{8}H_{21}^1 \frac{\lambda^1}{E_\pi^2} H_{21}^1 \eta H_{40}^2 \eta H_{21}^1 \frac{\lambda^1}{E_\pi^2} H_{21}^1 \\
& \left. + H_{21}^1 \frac{\lambda^1}{E_\pi} H_{21}^1 \frac{\lambda^2}{E_\pi} H_{21}^1 \frac{\lambda^1}{E_\pi} H_{40}^2 \frac{\lambda^1}{E_\pi} H_{21}^1 + \frac{1}{2}H_{21}^1 \frac{\lambda^1}{E_\pi} H_{21}^1 \frac{\lambda^2}{E_\pi} H_{40}^2 \frac{\lambda^2}{E_\pi} H_{21}^1 \frac{\lambda^1}{E_\pi} H_{21}^1 \right] \eta + \text{h.c.} \tag{3.46}
\end{aligned}$$

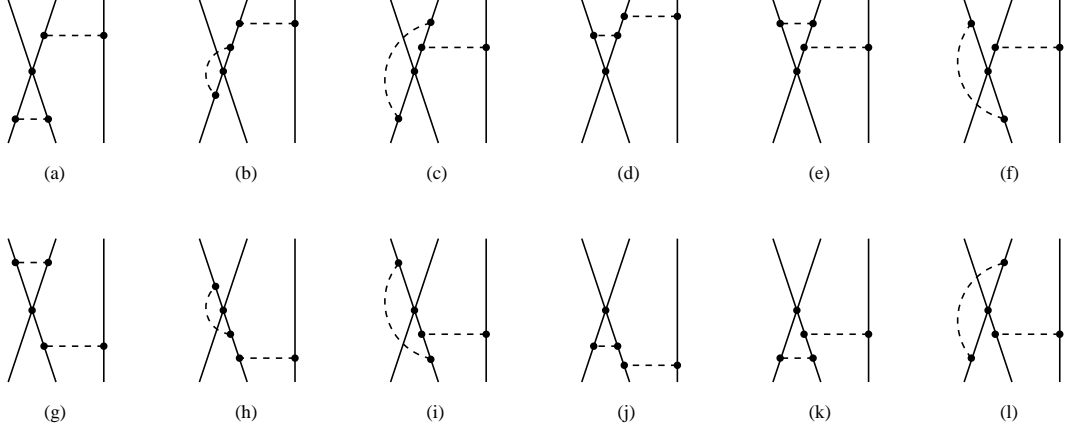


FIG. 9: Class-IV three-nucleon diagrams which do not involve self-energy insertions. For notation, see Figs. 1 and 2.

In addition to terms listed above one has to include contributions arising from the η -space unitary transformation defined in Eqs. (3.24), (3.25) and acting on H_{40}^2 ,⁴

$$\begin{aligned} \delta V^{(4)} = & \eta \left[\frac{1}{2} H_{21}^1 \frac{\lambda^1}{E_\pi} H_{21}^1 \eta H_{21}^1 \frac{\lambda^1}{E_\pi^3} H_{21}^1 \eta H_{40}^2 - \frac{1}{2} H_{21}^1 \frac{\lambda^1}{E_\pi^3} H_{21}^1 \eta H_{21}^1 \frac{\lambda^1}{E_\pi} H_{21}^1 \eta H_{40}^2 \right. \\ & \left. - \frac{1}{4} H_{21}^1 \frac{\lambda^1}{E_\pi} H_{21}^1 \frac{\lambda^2}{E_\pi} H_{21}^1 \frac{\lambda^1}{E_\pi^2} H_{21}^1 \eta H_{40}^2 + \frac{1}{4} H_{21}^1 \frac{\lambda^1}{E_\pi^2} H_{21}^1 \frac{\lambda^2}{E_\pi} H_{21}^1 \frac{\lambda^1}{E_\pi} H_{21}^1 \eta H_{40}^2 \right] \eta + \text{h.c.} \end{aligned} \quad (3.47)$$

Here, we already adopted the values for $\alpha_{1,2}$ from Eq. (3.31). Finally, one needs to take into account contributions which arise from yet unconsidered unitary transformation in Eq. (3.24) with $S = \alpha_6 S_6$ and the generator S_6 given by

$$S_6 = \eta \left[- H_{21}^1 \frac{\lambda^1}{E_\pi^3} H_{21}^1 \eta H_{40}^2 + H_{40}^2 \eta H_{21}^1 \frac{\lambda^1}{E_\pi^3} H_{21}^1 \right] \eta. \quad (3.48)$$

The corresponding contributions to the effective Hamilton operator read:

$$\begin{aligned} \delta V^{(4)} = & \alpha_6 \eta \left[H_{21}^1 \frac{\lambda^1}{E_\pi} H_{21}^1 \eta H_{21}^1 \frac{\lambda^1}{E_\pi^3} H_{21}^1 \eta H_{40}^2 + H_{40}^2 \eta H_{21}^1 \frac{\lambda^1}{E_\pi^3} H_{21}^1 \eta H_{21}^1 \frac{\lambda^1}{E_\pi} H_{21}^1 \right. \\ & \left. - H_{21}^1 \frac{\lambda^1}{E_\pi} H_{21}^1 \eta H_{40}^2 \eta H_{21}^1 \frac{\lambda^1}{E_\pi^3} H_{21}^1 - H_{21}^1 \frac{\lambda^1}{E_\pi^3} H_{21}^1 \eta H_{40}^2 \eta H_{21}^1 \frac{\lambda^1}{E_\pi} H_{21}^1 \right] \eta. \end{aligned} \quad (3.49)$$

Notice that the second possible generator

$$\eta \left[- H_{21}^1 \frac{\lambda^1}{E_\pi^2} H_{40}^2 \frac{\lambda^1}{E_\pi} H_{21}^1 + H_{21}^1 \frac{\lambda^1}{E_\pi} H_{40}^2 \frac{\lambda^1}{E_\pi^2} H_{21}^1 \right] \eta = 0 \quad (3.50)$$

does not lead to a non-trivial transformation. The constant α_6 can be determined unambiguously by the requirement that the OPEP factorizes out in the 3NF diagrams shown in Fig. 9. The energy denominators for the individual graphs in this figure read:

$$\bar{V}_{3N}^a = \bar{V}_{3N}^g = 2(1 - 2\alpha_6) \frac{\omega_i^2 + \omega_j^2}{\omega_i^3 \omega_j^3},$$

⁴ These terms are not shown explicitly in Eq. (3.27).

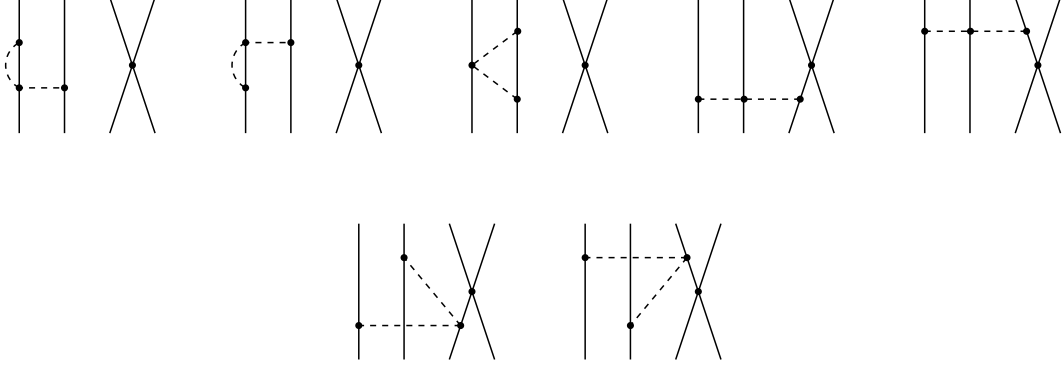


FIG. 10: Class-V contributions to the 4NF. For notation, see Figs. 1 and 2.

$$\begin{aligned}
\bar{V}_{3N}^b &= -\bar{V}_{3N}^c = \bar{V}_{3N}^h = -\bar{V}_{3N}^i = -\frac{2}{\omega_i \omega_j^3}, \\
\bar{V}_{3N}^d &= \bar{V}_{3N}^j = \frac{4\alpha_6}{\omega_i \omega_j^3}, \\
\bar{V}_{3N}^e &= \bar{V}_{3N}^k = -\frac{2}{\omega_i \omega_j^3} - 2(1 - 2\alpha_6) \frac{1}{\omega_i^3 \omega_j}, \\
\bar{V}_{3N}^f &= \bar{V}_{3N}^l = 0.
\end{aligned} \tag{3.51}$$

Here, i labels the pion exchanged between the first two nucleons and the third one while j denotes the pion which does not interact with the third nucleon. The OPEP factorizes out in the above terms if one sets

$$\alpha_6 = \frac{1}{2}. \tag{3.52}$$

We have verified that this choice also leads to the desired $1/\omega_i$ -dependence for the class-IV 3NF contributions involving self-energy insertions which are not shown in Fig. 9. With the η -space unitary transformations being fixed as described above only the last two diagrams in Fig. 8 yield non-vanishing 4NF contributions:

$$V_{\text{Class-IV}} = 4C_T \frac{g_A^4}{(2F_\pi)^4} \frac{\vec{\sigma}_1 \cdot \vec{q}_1 \vec{\sigma}_3 \times \vec{\sigma}_4 \cdot \vec{q}_{12}}{[\vec{q}_1^2 + M_\pi^2][\vec{q}_{12}^2 + M_\pi^2]^2} \left[\tau_1 \cdot \tau_3 \vec{q}_1 \times \vec{q}_{12} \cdot \vec{\sigma}_2 - \tau_1 \times \tau_2 \cdot \tau_3 \vec{q}_1 \cdot \vec{q}_{12} \right] + \text{all perm.} \tag{3.53}$$

- **Class-V** contributions proportional to $g_A^2 C_{S,T}$.

The class-V contributions arise from diagrams constructed from two vertices H_{21}^1 , one Weinberg-Tomozawa vertex H_{22}^2 and the leading contact interaction H_{40}^2 , see Fig. 10. From Eqs. (2.14)-(2.17), one obtains:

$$\begin{aligned}
V^{(4)} &= \eta \left[\frac{1}{2} H_{40}^2 \eta H_{21}^1 \frac{\lambda^1}{E_\pi} H_{21}^1 \frac{\lambda^2}{E_\pi^2} H_{22}^2 + \frac{1}{2} H_{40}^2 \eta H_{21}^1 \frac{\lambda^1}{E_\pi} H_{22}^2 \frac{\lambda^1}{E_\pi^2} H_{21}^1 + \frac{1}{2} H_{40}^2 \eta H_{22}^2 \frac{\lambda^2}{E_\pi} H_{21}^1 \frac{\lambda^1}{E_\pi^2} H_{21}^1 \right. \\
&+ \frac{1}{2} H_{40}^2 \eta H_{21}^1 \frac{\lambda^1}{E_\pi^2} H_{21}^1 \frac{\lambda^2}{E_\pi} H_{22}^2 + \frac{1}{2} H_{40}^2 \eta H_{21}^1 \frac{\lambda^1}{E_\pi^2} H_{22}^2 \frac{\lambda^1}{E_\pi} H_{21}^1 + \frac{1}{2} H_{40}^2 \eta H_{22}^2 \frac{\lambda^2}{E_\pi^2} H_{21}^1 \frac{\lambda^1}{E_\pi} H_{21}^1 \\
&\left. - H_{21}^1 \frac{\lambda^1}{E_\pi} H_{21}^1 \frac{\lambda^2}{E_\pi} H_{40}^2 \frac{\lambda^2}{E_\pi} H_{22}^2 - H_{21}^1 \frac{\lambda^1}{E_\pi} H_{22}^2 \frac{\lambda^1}{E_\pi} H_{40}^2 \frac{\lambda^1}{E_\pi} H_{21}^1 - H_{21}^1 \frac{\lambda^1}{E_\pi} H_{40}^2 \frac{\lambda^1}{E_\pi} H_{21}^1 \frac{\lambda^2}{E_\pi} H_{22}^2 \right] \eta + \text{h.c.} \tag{3.54}
\end{aligned}$$

In addition, one has to take into account the contributions arising from the η -space unitary transformations proportional to $\alpha_{3,4,5}$ and acting on H_{40}^2 :

$$\begin{aligned}
\delta V^{(4)} &= -\alpha_5 \eta \left[H_{40}^2 \eta H_{21}^1 \frac{\lambda^1}{E_\pi^2} H_{22}^2 \frac{\lambda^1}{E_\pi} H_{21}^1 - H_{40}^2 \eta H_{21}^1 \frac{\lambda^1}{E_\pi} H_{22}^2 \frac{\lambda^1}{E_\pi^2} H_{21}^1 \right] \eta \\
&+ \left(\frac{1}{2} + 2\alpha_5 \right) \eta \left[H_{40}^2 \eta H_{22}^2 \frac{\lambda^2}{E_\pi^2} H_{21}^1 \frac{\lambda^1}{E_\pi} H_{21}^1 - H_{40}^2 \eta H_{21}^1 \frac{\lambda^1}{E_\pi} H_{21}^1 \frac{\lambda^2}{E_\pi^2} H_{22}^2 \right] \eta
\end{aligned}$$

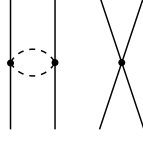


FIG. 11: Class-VI contribution to the 4NF. For notation, see Figs. 1 and 2.

$$+ \alpha_5 \eta \left[H_{40}^2 \eta H_{22}^2 \frac{\lambda^2}{E_\pi} H_{21}^1 \frac{\lambda^1}{E_\pi^2} H_{21}^1 - H_{40}^2 \eta H_{21}^1 \frac{\lambda^1}{E_\pi^2} H_{21}^1 \frac{\lambda^2}{E_\pi} H_{22}^2 \right] \eta + \text{h.c.} . \quad (3.55)$$

Here, we have adopted the values for $\alpha_{3,4}$ from Eq. (3.40). Similar to the class-II forces, the resulting 4NF turns out to be α_5 -independent. From the diagrams shown in Fig. 10, only the last two in the first row generate the non-vanishing contribution which reads:

$$V_{\text{Class-V}} = 2C_T \frac{g_A^2}{(2F_\pi)^4} \frac{\vec{\sigma}_1 \cdot \vec{q}_1 \vec{\sigma}_3 \times \vec{\sigma}_4 \cdot \vec{q}_{12}}{[\vec{q}_1^2 + M_\pi^2][\vec{q}_{12}^2 + M_\pi^2]} \boldsymbol{\tau}_1 \times \boldsymbol{\tau}_2 \cdot \boldsymbol{\tau}_3 + \text{all perm.} . \quad (3.56)$$

- **Class-VI** contributions proportional to $C_{S,T}$.

The only way the class-VI contributions can be generated is from a single disconnected diagram shown in Fig. 11. The corresponding terms in the effective potential read:

$$V^{(4)} = \eta \left[\frac{1}{2} H_{22}^2 \frac{\lambda^2}{E_\pi} H_{40}^2 \frac{\lambda^2}{E_\pi} H_{22}^2 - \frac{1}{2} H_{22}^2 \frac{\lambda^2}{E_\pi^2} H_{22}^2 \eta H_{40}^2 \right] \eta + \text{h.c.} . \quad (3.57)$$

It is easy to verify that the diagram in Fig. 11 leads to a vanishing 4NF.

- **Class-VII** contributions proportional to $g_A^2 C_{S,T}^2$.

The class-VII contributions arise from diagrams involving two vertices H_{21}^1 and two insertions of the leading-order contact interactions H_{40}^2 , see Fig. 12. From Eqs. (2.14)-(2.17), one obtains:

$$V^{(4)} = \eta \left[-\frac{1}{2} H_{21}^1 \frac{\lambda^1}{\omega} H_{40}^2 \frac{\lambda^1}{\omega} H_{40}^2 \frac{\lambda^1}{\omega} H_{21}^1 + \frac{1}{2} H_{21}^1 \frac{\lambda^1}{\omega} H_{40}^2 \frac{\lambda^1}{\omega^2} H_{21}^1 \eta H_{40}^2 + \frac{1}{2} H_{21}^1 \frac{\lambda^1}{\omega^2} H_{40}^2 \frac{\lambda^1}{\omega} H_{21}^1 \eta H_{40}^2 - \frac{1}{2} H_{21}^1 \frac{\lambda^1}{\omega^3} H_{21}^1 \eta H_{40}^2 \eta H_{40}^2 \right] \eta + \text{h.c.} . \quad (3.58)$$

Further terms arise from the η -space unitary transformation proportional to α_6 , see Eq. (3.48), and acting on H_{40}^2 . Using the value for α_6 from Eq. (3.52), these contributions take the form:

$$\delta V^{(4)} = \eta \left[-H_{40}^2 \eta H_{21}^1 \frac{\lambda^1}{E_\pi^3} H_{21}^1 \eta H_{40}^2 + \frac{1}{2} H_{40}^2 \eta H_{40}^2 \eta H_{21}^1 \frac{\lambda^1}{E_\pi^3} H_{21}^1 + \frac{1}{2} H_{21}^1 \frac{\lambda^1}{E_\pi^3} H_{21}^1 \eta H_{40}^2 \eta H_{40}^2 \right] \eta . \quad (3.59)$$

From all diagrams shown in Fig. 12, only the third, fourth and fifth ones in the second row lead to the nonvanishing 4NF:

$$V_{\text{Class-VII}} = 2C_T^2 \frac{g_A^2}{(2F_\pi)^2} \frac{\vec{\sigma}_1 \times \vec{\sigma}_2 \cdot \vec{q}_{12} \vec{\sigma}_3 \times \vec{\sigma}_4 \cdot \vec{q}_{12}}{[\vec{q}_{12}^2 + M_\pi^2]^2} \boldsymbol{\tau}_2 \cdot \boldsymbol{\tau}_3 + \text{all perm.} . \quad (3.60)$$

- **Class-VIII** contributions from disconnected graphs with insertions of a $\Delta_i = 2$ -interaction.

Finally, we need to consider contributions involving insertions of the $\Delta_i = 2$ -interactions H_{20}^2 , H_{02}^2 , H_{21}^3 and H_{40}^4 and arising from disconnected diagrams shown in Fig. 13. The corresponding terms in the effective Hamilton operator are listed in Appendix A. Evaluating matrix elements of these terms we have verified that all disconnected diagrams in Fig. 13 lead to vanishing contributions to the 4NF.

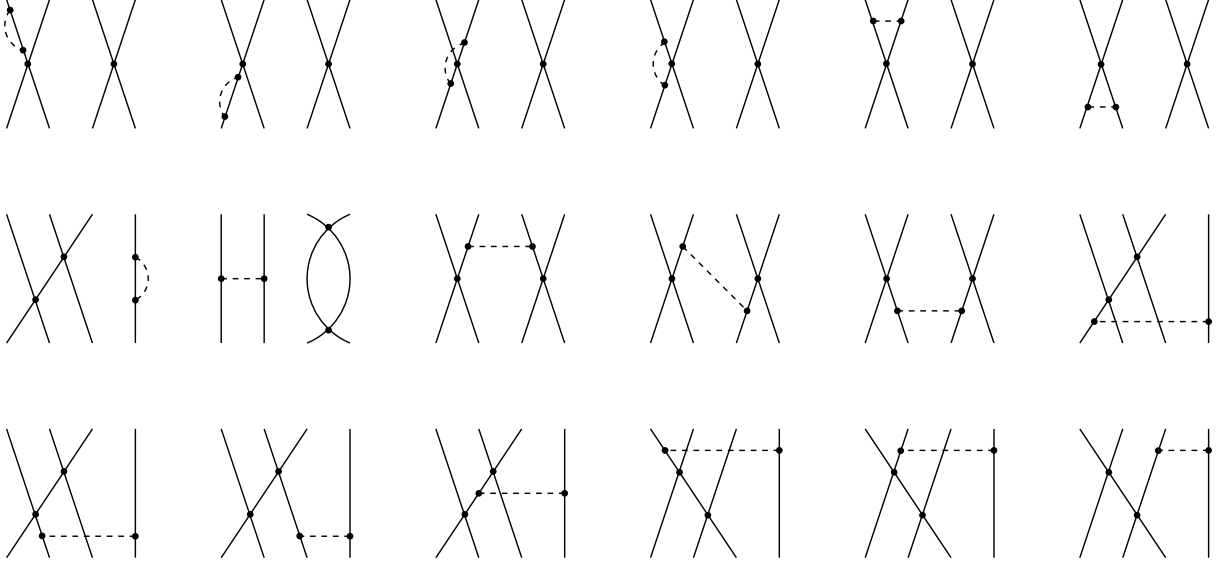


FIG. 12: Class-VII contributions to the 4NF. For notation, see Figs. 1 and 2.

D. Discussion

In the previous section we have worked out the leading 4NF which is given in Eqs. (3.33), (3.41), (3.44), (3.53), (3.56) and (3.60). Some of these contributions have, in fact, already been considered in the past. In particular, McManus and Riska [29] discussed a long time ago the 4NF generated by the last two diagrams in Fig. 5. These terms were also studied by Robilotta [30] who, in addition, considered effects due to intermediate delta excitations and exchange of rho and axial-vector mesons. In that work, the $\pi\pi\pi NN$ and $\pi\pi\pi\pi$ vertices were parametrized in terms of the constant ξ which plays a role similar to α in Eq. (3.19). Our result for the penultimate diagram in Fig. 5 shown in the first line of Eq. (3.44) agrees with the one of Ref. [29] if one chooses $\alpha = 1/4$ and with the one of Ref. [30] if one chooses $4\alpha = \xi$. The result for the last diagram in Fig. 5 which is given in the last two lines of Eq. (3.44) does, however, only agree with the one of Ref. [30] if one sets $\alpha = \xi = 0$, see Eq. (43) of that work. This disagreement can be traced back to the (slightly) different Feynman rules used for the $\pi\pi\pi\pi$ vertex in that work. Notice further that the ξ -dependence does not drop out completely in the expressions for the 4NF of Ref. [30]. All other nonvanishing 4NF contributions discussed in the previous section result from diagrams involving reducible topologies and have, to the best of our knowledge, not been considered before.

In order to test the effects of the 4NFs in few-nucleon systems explicit calculations will need to be performed. To get a rough idea about the size of the 4NF contributions to e.g. the α -particle binding energy, one can look at the strength of the corresponding r -space potentials which are given in appendix B. The strengths of the contributions which do not involve contact interactions is given by

$$\frac{g_A^6 M_\pi^7}{(16\pi F_\pi^2)^3} \sim 50 \text{ keV} \quad \text{and} \quad \frac{g_A^4 M_\pi^7}{(16\pi F_\pi^2)^3} \sim 35 \text{ keV}, \quad (3.61)$$

see also [30]. These numbers set the typical scale for the expectation values of the corresponding operators. Recently, a more careful estimation of the 4NF effects in ${}^4\text{He}$ was carried out by Rozpedzik et al. [31] which, however, still involves severe approximations in order to simplify the calculations. Expectation values of various individual long-range 4NF contributions (i.e. the ones which do not involve contact interactions) obtained in that work agree reasonably well with the above estimation. For example, for the Gaussian wave function their magnitudes lie in the range $\sim 70 \dots 200$ keV. Interestingly, one observes strong cancellations among various contributions. The cancellation (to a large extent) between the contributions corresponding to the last two diagrams in Fig. 5 was already mentioned in Ref. [29]. Even

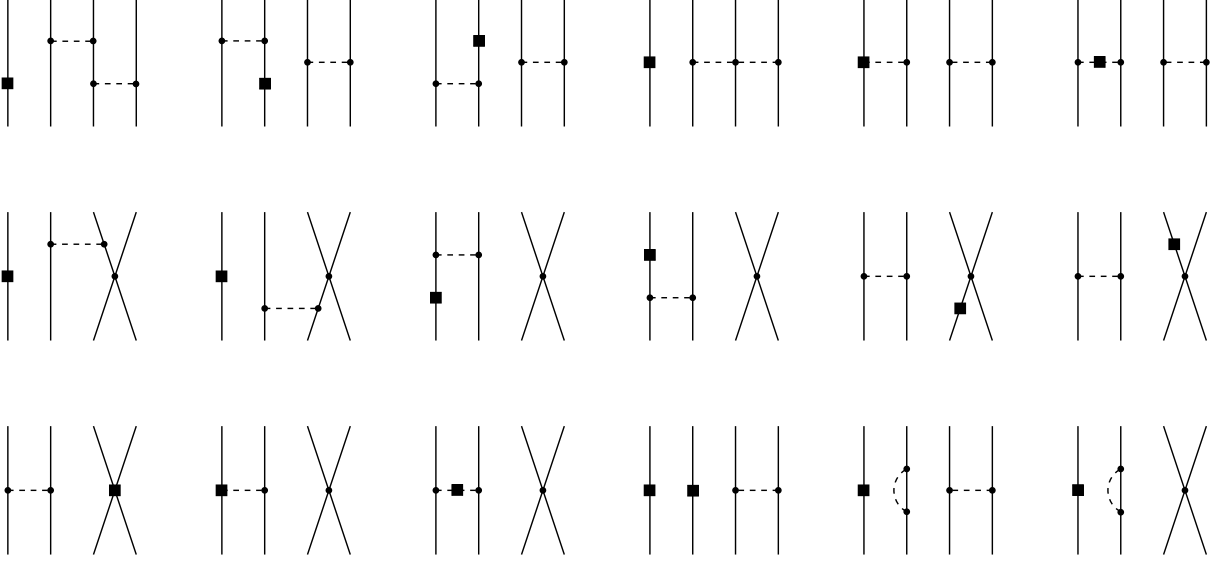


FIG. 13: Class-VIII contributions to the 4NF. Solid squares denote vertices of order $\nu = 4$. For the remaining notation see Figs. 1 and 2.

more surprising, one observes a nearly complete cancellation for the total long-range contribution $V_{\text{Class-I}} + V_{\text{Class-II}}$.⁵ For all three wave functions employed in Ref. [31], its expectation value does not exceed 4 keV. Further, a similar cancellation occurs for the class-IV and class-V contributions. For the Gaussian wave function, the corresponding expectation values are [31]

$$\langle \Psi_{^4\text{He}} | V_{\text{Class-IV}} | \Psi_{^4\text{He}} \rangle + \langle \Psi_{^4\text{He}} | V_{\text{Class-V}} | \Psi_{^4\text{He}} \rangle = (14.2 \text{ keV}) \times C_T - (14.9 \text{ keV}) \times C_T. \quad (3.62)$$

Here the value for the LEC C_T should be taken in units of GeV^{-2} . The LEC C_T has been determined from fits to NN phase shifts. Its value depends on the cutoffs employed and is typically of the order $|C_T| \sim 10 \text{ GeV}^{-2}$ [2]. Values obtained from resonance saturation using various phenomenological potentials are of a similar size [32]. One therefore concludes that the contribution to the ^4He binding energy from 4NF terms proportional to C_T is rather small. The most significant contribution is produced by the class-VII 4NF which is quadratic in C_T . For the Gaussian wave function it is found to be [31]

$$\langle \Psi_{^4\text{He}} | V_{\text{Class-VII}} | \Psi_{^4\text{He}} \rangle = (-1.1 \text{ keV}) \times C_T^2. \quad (3.63)$$

For $|C_T| \sim 10 \text{ GeV}^{-2}$ the 4NF is, therefore, expected to produce $\sim 100 \text{ keV}$ attraction in ^4He . We, however, emphasize that the expectation values for the contributions involving contact interactions might be significantly overestimated due to approximations made in Ref. [31] for the ^4He wave functions [33].

IV. SUMMARY AND CONCLUSIONS

In this paper we have analyzed the next-to-next-to-next-to-leading contribution to the nuclear Hamiltonian in chiral effective field theory using the method of unitary transformation. The pertinent results can be summarized as follows:

- i) We have presented a new formulation of the chiral power counting which is particularly suitable for applications based on algebraic approaches such as the method of unitary transformation. It allowed us to express the

⁵ Expressions for V^c and V^l in Refs. [11] and [31] should be taken with opposite sign.

recursive (formal) solution of the decoupling equation in a compact form and to drastically simplify the derivation of the effective Hamiltonian as compared to the formalism given in Ref. [12].

- ii) Using this new formulation we have worked out the N³LO contribution to the effective nuclear Hamiltonian in chiral EFT which involves 2N, 3N and 4N operators. The 4N operators yield the leading contribution to the 4NF.
- iii) We employed a large class of additional η -space unitary transformations that affect N³LO terms in the effective Hamiltonian. The appearance of such transformations is a new feature at this order in the chiral expansion. We found that certain classes of the 3NF at N³LO cannot be renormalized for an arbitrary choice of the η -space transformations. The renormalizability requirement leads to constraints for these additional unitary transformations but does not fix them completely.
- iv) We have worked out the leading 4NF both in momentum and configuration spaces. Enforcing the above mentioned renormalizability constraints we found no ambiguity in the 4NF due to the employed η -space unitary transformations. The resulting 4NF is local and depends on the pion decay constant F_π , the axial pion-nucleon coupling g_A and the lowest-order NN contact interaction whose strength C_T is determined in the two-nucleon system [3, 4].

In the future, the effects of the 4NF should be tested in the four-nucleon continuum and in the spectra of light nuclei. Further, it is also important to study effects due to intermediate delta excitations which are expected to be significant [30]. Work along these lines is in progress.

Acknowledgements

We are grateful to Hermann Krebs and Ulf-G. Meißner for helpful discussions and useful comments on the manuscript. This work was supported by the Helmholtz Association under the contract number VH-NG-222.

APPENDIX A: CONTRIBUTIONS OF THE ORDER $\Delta_i = 2$ VERTICES TO THE EFFECTIVE HAMILTON OPERATOR AT ORDER $\nu = 4$

In this appendix we consider the operator structure of the effective Hamiltonian at order $\nu = 4$ which results from higher-order vertices. As already pointed out, these terms lead to disconnected diagrams which are shown in Fig. 13. As a general rule, such disconnected diagrams do not yield nonvanishing contributions to the effective Hamilton operator in the method of unitary transformation. For the sake of completeness, we list below the complete operator structure of the class-VIII contributions. The relevant vertices at order $\Delta_i = 2$ are H_{20}^2 , H_{02}^2 , H_{21}^3 and H_{40}^4 . The interaction H_{02}^2 together with the corresponding pion tadpole diagrams renormalize the pion mass and wave function. As discussed in [21], the H_{02}^2 vertex does not show up provided the Lagrangian is formulated in terms of renormalized pion fields and normal ordering is applied. We will, therefore, not consider the contributions involving H_{02}^2 in what follows.

Let us begin with the contributions which involve insertions of the nucleon kinetic energy H_{20}^2 . Using the values for α_i from Eqs. (3.31), (3.40) and (3.52) one obtains

- terms $\propto g_A^4$:

$$\begin{aligned}
 V = & \eta \left[\frac{1}{2} H_{21}^1 \frac{\lambda^1}{E_\pi} H_{21}^1 \eta H_{21}^1 \frac{\lambda^1}{E_\pi^3} H_{21}^1 \eta H_{20}^2 - H_{21}^1 \frac{\lambda^1}{E_\pi} H_{21}^1 \eta H_{21}^1 \frac{\lambda^1}{E_\pi^3} H_{20}^2 \lambda^1 H_{21}^1 \right. \\
 & + \frac{1}{2} H_{21}^1 \frac{\lambda^1}{E_\pi} H_{21}^1 \eta H_{20}^2 \eta H_{21}^1 \frac{\lambda^1}{E_\pi^3} H_{21}^1 - \frac{3}{4} H_{21}^1 \frac{\lambda^1}{E_\pi} H_{21}^1 \frac{\lambda^2}{E_\pi} H_{21}^1 \frac{\lambda^1}{E_\pi^2} H_{21}^1 \eta H_{20}^2 \\
 & \left. + H_{21}^1 \frac{\lambda^1}{E_\pi} H_{21}^1 \frac{\lambda^2}{E_\pi} H_{21}^1 \frac{\lambda^1}{E_\pi^2} H_{20}^2 \lambda^1 H_{21}^1 - \frac{1}{2} H_{21}^1 \frac{\lambda^1}{E_\pi} H_{21}^1 \frac{\lambda^2}{E_\pi^2} H_{21}^1 \frac{\lambda^1}{E_\pi} H_{21}^1 \eta H_{20}^2 \right]
 \end{aligned}$$

$$\begin{aligned}
& + \frac{1}{2} H_{21}^1 \frac{\lambda^1}{E_\pi} H_{21}^1 \frac{\lambda^2}{E_\pi^2} H_{20}^2 \lambda^2 H_{21}^1 \frac{\lambda^1}{E_\pi} H_{21}^1 + \frac{3}{8} H_{21}^1 \frac{\lambda^1}{E_\pi^2} H_{21}^1 \eta H_{21}^1 \frac{\lambda^1}{E_\pi^2} H_{21}^1 \eta H_{20}^2 \\
& - \frac{1}{2} H_{21}^1 \frac{\lambda^1}{E_\pi^2} H_{21}^1 \eta H_{21}^1 \frac{\lambda^1}{E_\pi^2} H_{20}^2 \lambda^1 H_{21}^1 + \frac{1}{8} H_{21}^1 \frac{\lambda^1}{E_\pi^2} H_{21}^1 \eta H_{20}^2 \eta H_{21}^1 \frac{\lambda^1}{E_\pi^2} H_{21}^1 \\
& - \frac{1}{4} H_{21}^1 \frac{\lambda^1}{E_\pi^2} H_{21}^1 \frac{\lambda^2}{E_\pi} H_{21}^1 \frac{\lambda^1}{E_\pi^2} H_{21}^1 \eta H_{20}^2 \Big] \eta + \text{h.c.}, \tag{A.1}
\end{aligned}$$

- terms $\propto g_A^2$:

$$\begin{aligned}
V = & \eta \left[(1 + 2\alpha_5) H_{21}^1 \frac{\lambda^1}{E_\pi} H_{21}^1 \frac{\lambda^2}{E_\pi^2} H_{22}^2 \eta H_{20}^2 - H_{21}^1 \frac{\lambda^1}{E_\pi} H_{21}^1 \frac{\lambda^2}{E_\pi^2} H_{20}^2 \lambda^2 H_{22}^2 \right. \\
& + \frac{1}{2} (1 - 2\alpha_5) H_{21}^1 \frac{\lambda^1}{E_\pi} H_{22}^2 \frac{\lambda^1}{E_\pi^2} H_{21}^1 \eta H_{20}^2 - H_{21}^1 \frac{\lambda^1}{E_\pi} H_{22}^2 \frac{\lambda^1}{E_\pi^2} H_{20}^2 \lambda^1 H_{21}^1 \\
& + \frac{1}{2} (1 + 2\alpha_5) H_{21}^1 \frac{\lambda^1}{E_\pi^2} H_{21}^1 \frac{\lambda^2}{E_\pi} H_{22}^2 \eta H_{20}^2 + \frac{1}{2} (1 + 2\alpha_5) H_{21}^1 \frac{\lambda^1}{E_\pi^2} H_{22}^2 \frac{\lambda^1}{E_\pi} H_{21}^1 \eta H_{20}^2 \\
& - H_{21}^1 \frac{\lambda^1}{E_\pi^2} H_{20}^2 \lambda^1 H_{21}^1 \frac{\lambda^2}{E_\pi} H_{22}^2 - 2\alpha_5 H_{22}^2 \frac{\lambda^2}{E_\pi^2} H_{21}^1 \frac{\lambda^1}{E_\pi} H_{21}^1 \eta H_{20}^2 \\
& + \frac{1}{2} (1 - 2\alpha_5) H_{22}^2 \frac{\lambda^2}{E_\pi} H_{21}^1 \frac{\lambda^1}{E_\pi^2} H_{21}^1 \eta H_{20}^2 - \frac{1}{2} H_{21}^1 \frac{\lambda^1}{E_\pi^3} H_{21}^1 \eta H_{20}^2 \eta H_{20}^2 \\
& \left. + H_{21}^1 \frac{\lambda^1}{E_\pi^3} H_{20}^2 \lambda^1 H_{21}^1 \eta H_{20}^2 - \frac{1}{2} H_{21}^1 \frac{\lambda^1}{E_\pi^3} H_{20}^2 \lambda^1 H_{20}^2 \lambda^1 H_{21}^1 \right] \eta + \text{h.c.}, \tag{A.2}
\end{aligned}$$

- terms $\propto g_A^2 C_{S,T}$:

$$\begin{aligned}
V = & \eta \left[\frac{1}{2} H_{21}^1 \frac{\lambda^1}{E_\pi} H_{40}^2 \frac{\lambda^1}{E_\pi^2} H_{21}^1 \eta H_{20}^2 - H_{21}^1 \frac{\lambda^1}{E_\pi} H_{40}^2 \frac{\lambda^1}{E_\pi^2} H_{20}^2 \lambda^1 H_{21}^1 + \frac{1}{2} H_{21}^1 \frac{\lambda^1}{E_\pi^2} H_{40}^2 \frac{\lambda^1}{E_\pi} H_{21}^1 \eta H_{20}^2 \right. \\
& \left. - \frac{1}{2} H_{21}^1 \frac{\lambda^1}{E_\pi^3} H_{21}^1 \eta H_{20}^2 \eta H_{40}^2 + H_{21}^1 \frac{\lambda^1}{E_\pi^3} H_{20}^2 \lambda^1 H_{21}^1 \eta H_{40}^2 - \frac{1}{2} H_{40}^2 \eta H_{21}^1 \frac{\lambda^1}{E_\pi^3} H_{21}^1 \eta H_{20}^2 \right] \eta + \text{h.c.}. \tag{A.3}
\end{aligned}$$

It should be emphasized that one can construct η -space unitary transformations with the generators depending on H_{20}^2 . Such transformations would produce further contributions which are not considered here.

Next consider the operators which involve one insertion of the subleading pion-nucleon vertex H_{21}^3 . One obtains

- terms $\propto g_A^3$:

$$\begin{aligned}
V = & \eta \left[\frac{1}{2} H_{21}^1 \frac{\lambda^1}{E_\pi} H_{21}^1 \eta H_{21}^1 \frac{\lambda^1}{E_\pi^2} H_{21}^3 + \frac{1}{2} H_{21}^1 \frac{\lambda^1}{E_\pi} H_{21}^1 \eta H_{21}^3 \frac{\lambda^1}{E_\pi^2} H_{21}^1 - H_{21}^1 \frac{\lambda^1}{E_\pi} H_{21}^1 \frac{\lambda^2}{E_\pi} H_{21}^1 \frac{\lambda^1}{E_\pi} H_{21}^3 \right. \\
& \left. - H_{21}^1 \frac{\lambda^1}{E_\pi} H_{21}^1 \frac{\lambda^2}{E_\pi} H_{21}^3 \frac{\lambda^1}{E_\pi} H_{21}^1 + \frac{1}{2} H_{21}^1 \frac{\lambda^1}{E_\pi^2} H_{21}^1 \eta H_{21}^1 \frac{\lambda^1}{E_\pi} H_{21}^3 + \frac{1}{2} H_{21}^1 \frac{\lambda^1}{E_\pi^2} H_{21}^1 \eta H_{21}^3 \frac{\lambda^1}{E_\pi} H_{21}^1 \right] \eta + \text{h.c.}, \tag{A.4}
\end{aligned}$$

- terms $\propto g_A C_{S,T}$:

$$V = \eta \left[H_{21}^1 \frac{\lambda^1}{E_\pi} H_{40}^2 \frac{\lambda^1}{E_\pi} H_{21}^3 - \frac{1}{2} H_{21}^1 \frac{\lambda^1}{E_\pi^2} H_{21}^3 \eta H_{40}^2 - \frac{1}{2} H_{21}^3 \frac{\lambda^1}{E_\pi^2} H_{21}^1 \eta H_{40}^2 \right] \eta + \text{h.c.}. \tag{A.5}$$

Finally, the contributions involving H_{40}^4 read:

$$V = \eta \left[H_{21}^1 \frac{\lambda^1}{E_\pi} H_{40}^4 \frac{\lambda^1}{E_\pi} H_{21}^1 - \frac{1}{2} H_{21}^1 \frac{\lambda^1}{E_\pi^2} H_{21}^1 \eta H_{40}^4 - \frac{1}{2} H_{40}^4 \eta H_{21}^1 \frac{\lambda^1}{E_\pi^2} H_{21}^1 \right] \eta. \tag{A.6}$$

We have verified via explicit calculations that matrix elements of all terms listed above and corresponding to 4N diagrams shown in Fig. 13 vanish.

APPENDIX B: CONFIGURATION-SPACE REPRESENTATION OF THE FOUR-NUCLEON FORCE

The derived expressions for the 4NF depend only on the momentum transfer of the nucleons and, therefore, take the local form in the configuration space:

$$\langle \vec{r}'_1 \vec{r}'_2 \vec{r}'_3 \vec{r}'_4 | V_{4N} | \vec{r}_1 \vec{r}_2 \vec{r}_3 \vec{r}_4 \rangle = \delta(\vec{r}'_1 - \vec{r}_1) \delta(\vec{r}'_2 - \vec{r}_2) \delta(\vec{r}'_3 - \vec{r}_3) \delta(\vec{r}'_4 - \vec{r}_4) V_{4N}. \quad (\text{B.1})$$

Clearly, the locality of the 4NF only holds if one uses a regulator function which depends on momentum transfers \vec{q}_i as well. In this appendix we give the configuration-space representation of the 4NF for a general form of a local regulator.

Depending on the topology, the 4NF is expressed in Eqs. (3.33), (3.41), (3.44), (3.53), (3.56) and (3.60) in terms of different sets of momenta, namely $\{\vec{q}_2, \vec{q}_3, \vec{q}_4\}$, $\{\vec{q}_1, \vec{q}_{12}, \vec{q}_4\}$ and $\{\vec{q}_1, \vec{q}_2, \vec{q}_3, \vec{q}_4\}$. The corresponding configuration-space expressions have the form:

$$\begin{aligned} V_{4N} &= \int \frac{d^3 q_2}{(2\pi)^3} \frac{d^3 q_3}{(2\pi)^3} \frac{d^3 q_4}{(2\pi)^3} e^{i\vec{q}_2 \cdot \vec{r}_{21}} e^{i\vec{q}_3 \cdot \vec{r}_{31}} e^{i\vec{q}_4 \cdot \vec{r}_{41}} V_{4N}(\vec{q}_2, \vec{q}_3, \vec{q}_4), \\ V_{4N} &= \int \frac{d^3 q_1}{(2\pi)^3} \frac{d^3 q_{12}}{(2\pi)^3} \frac{d^3 q_4}{(2\pi)^3} e^{i\vec{q}_1 \cdot \vec{r}_{12}} e^{i\vec{q}_{12} \cdot \vec{r}_{23}} e^{i\vec{q}_4 \cdot \vec{r}_{43}} V_{4N}(\vec{q}_1, \vec{q}_{12}, \vec{q}_4), \\ V_{4N} &= \int d^3 r_0 \int \frac{d^3 q_1}{(2\pi)^3} \frac{d^3 q_2}{(2\pi)^3} \frac{d^3 q_3}{(2\pi)^3} \frac{d^3 q_4}{(2\pi)^3} e^{i\vec{q}_1 \cdot \vec{r}_{10}} e^{i\vec{q}_2 \cdot \vec{r}_{20}} e^{i\vec{q}_3 \cdot \vec{r}_{30}} e^{i\vec{q}_4 \cdot \vec{r}_{40}} V_{4N}(\vec{q}_2, \vec{q}_2, \vec{q}_3, \vec{q}_4), \end{aligned} \quad (\text{B.2})$$

where $\vec{r}'_{ij} \equiv \vec{r}'_i - \vec{r}'_j$. Here we have taken into account the overall factor $(2\pi)^3 \delta(\vec{P}' - \vec{P})$ with \vec{P} and \vec{P}' being the total initial and final momenta of the nucleons, which is not shown explicitly in expressions of sec. III C. Using Eq. (B.2) we obtain:

$$\begin{aligned} V_{\text{Class-I}} &= \frac{g_A^6 M_\pi^7}{(16\pi F_\pi^2)^3} \vec{\sigma}_1 \cdot \vec{\nabla}_{12} \vec{\sigma}_4 \cdot \vec{\nabla}_{43} \left[(\boldsymbol{\tau}_1 \cdot \boldsymbol{\tau}_4 \boldsymbol{\tau}_2 \cdot \boldsymbol{\tau}_3 - \boldsymbol{\tau}_1 \cdot \boldsymbol{\tau}_3 \boldsymbol{\tau}_2 \cdot \boldsymbol{\tau}_4) \vec{\nabla}_{12} \cdot \vec{\nabla}_{23} \vec{\nabla}_{43} \cdot \vec{\nabla}_{23} \right. \\ &\quad + \boldsymbol{\tau}_1 \times \boldsymbol{\tau}_2 \cdot \boldsymbol{\tau}_4 \vec{\nabla}_{12} \cdot \vec{\nabla}_{23} \vec{\nabla}_{23} \times \vec{\nabla}_{43} \cdot \vec{\sigma}_3 + \boldsymbol{\tau}_1 \times \boldsymbol{\tau}_3 \cdot \boldsymbol{\tau}_4 \vec{\nabla}_{43} \cdot \vec{\nabla}_{23} \vec{\nabla}_{12} \times \vec{\nabla}_{23} \cdot \vec{\sigma}_2 \\ &\quad \left. + \boldsymbol{\tau}_1 \cdot \boldsymbol{\tau}_4 \vec{\nabla}_{23} \times \vec{\nabla}_{12} \cdot \vec{\sigma}_2 \vec{\nabla}_{23} \times \vec{\nabla}_{43} \cdot \vec{\sigma}_3 \right] U_1(x_{12}) U_2(x_{23}) U_1(x_{43}) + \text{all perm.}, \\ V_{\text{Class-II}} &= \frac{2g_A^4 M_\pi^7}{(16\pi F_\pi^2)^3} \vec{\sigma}_1 \cdot \vec{\nabla}_{12} \vec{\sigma}_4 \cdot \vec{\nabla}_{43} \left[(\boldsymbol{\tau}_1 \cdot \boldsymbol{\tau}_4 \boldsymbol{\tau}_2 \cdot \boldsymbol{\tau}_3 - \boldsymbol{\tau}_1 \cdot \boldsymbol{\tau}_3 \boldsymbol{\tau}_2 \cdot \boldsymbol{\tau}_4) \vec{\nabla}_{23} \cdot \vec{\nabla}_{43} + \boldsymbol{\tau}_1 \times \boldsymbol{\tau}_2 \cdot \boldsymbol{\tau}_4 \vec{\nabla}_{23} \times \vec{\nabla}_{43} \cdot \vec{\sigma}_3 \right] \\ &\quad \times U_1(x_{12}) U_1(x_{23}) U_1(x_{43}) \\ &\quad + \frac{g_A^4 M_\pi^7}{(16\pi F_\pi^2)^3} \boldsymbol{\tau}_1 \cdot \boldsymbol{\tau}_2 \boldsymbol{\tau}_3 \cdot \boldsymbol{\tau}_4 \vec{\sigma}_2 \cdot \vec{\nabla}_{21} \vec{\sigma}_3 \cdot \vec{\nabla}_{31} \vec{\sigma}_4 \cdot \vec{\nabla}_{41} \vec{\sigma}_1 \cdot (\vec{\nabla}_{31} + \vec{\nabla}_{41}) U_1(x_{21}) U_1(x_{31}) U_1(x_{41}) \\ &\quad + \frac{g_A^4 M_\pi^7}{8\pi(16\pi F_\pi^2)^3} \boldsymbol{\tau}_1 \cdot \boldsymbol{\tau}_2 \boldsymbol{\tau}_3 \cdot \boldsymbol{\tau}_4 (1 - \vec{\nabla}_1^2 - \vec{\nabla}_2^2 - 2\vec{\nabla}_1 \cdot \vec{\nabla}_2) \vec{\sigma}_1 \cdot \vec{\nabla}_1 \vec{\sigma}_2 \cdot \vec{\nabla}_2 \vec{\sigma}_3 \cdot \vec{\nabla}_3 \vec{\sigma}_4 \cdot \vec{\nabla}_4 \\ &\quad \times \int d^3 x_0 U_1(x_{10}) U_1(x_{20}) U_1(x_{30}) U_1(x_{40}) + \text{all perm.}, \\ V_{\text{Class-IV}} &= \frac{2g_A^4 C_T M_\pi^7}{(16\pi F_\pi^2)^2} \vec{\sigma}_1 \cdot \vec{\nabla}_{12} \vec{\sigma}_3 \times \vec{\sigma}_4 \cdot \vec{\nabla}_{23} \left[\boldsymbol{\tau}_1 \cdot \boldsymbol{\tau}_3 \vec{\nabla}_{12} \times \vec{\nabla}_{23} \cdot \vec{\sigma}_2 - \boldsymbol{\tau}_1 \times \boldsymbol{\tau}_2 \cdot \boldsymbol{\tau}_3 \vec{\nabla}_{12} \cdot \vec{\nabla}_{23} \right] \\ &\quad \times U_1(x_{12}) U_2(x_{23}) W(x_{43}) + \text{all perm.}, \\ V_{\text{Class-V}} &= -\frac{2g_A^2 C_T M_\pi^7}{(16\pi F_\pi^2)^2} \boldsymbol{\tau}_1 \times \boldsymbol{\tau}_2 \cdot \boldsymbol{\tau}_3 \vec{\sigma}_1 \cdot \vec{\nabla}_{12} \vec{\sigma}_3 \times \vec{\sigma}_4 \cdot \vec{\nabla}_{23} U_1(x_{12}) U_1(x_{23}) W(x_{43}) + \text{all perm.}, \\ V_{\text{Class-VII}} &= -\frac{g_A^2 C_T^2 M_\pi^7}{16\pi F_\pi^2} \boldsymbol{\tau}_2 \cdot \boldsymbol{\tau}_3 \vec{\sigma}_1 \times \vec{\sigma}_2 \cdot \vec{\nabla}_{23} \vec{\sigma}_3 \times \vec{\sigma}_4 \cdot \vec{\nabla}_{23} W(x_{12}) U_1(x_{23}) W(x_{43}) + \text{all perm.} \end{aligned} \quad (\text{B.3})$$

Here, $\vec{x}_i \equiv M_\pi \vec{r}_i$, $\vec{x}_{ij} \equiv \vec{x}_i - \vec{x}_j$, $\vec{\nabla}_i$ ($\vec{\nabla}_{ij}$) acts on \vec{x}_i (\vec{x}_{ij}) and $x_{ij} \equiv |\vec{x}_{ij}|$. Further, the functions $U_{1,2}$ and W are defined as:

$$U_1(x_{ij}) = \frac{4\pi}{M_\pi} \int \frac{d^3 q}{(2\pi)^3} \frac{e^{i\vec{q} \cdot \vec{x}_{ij}/M_\pi}}{q^2 + M_\pi^2} F_1^\Lambda(q) \xrightarrow{\Lambda \rightarrow \infty} \frac{e^{-x_{ij}}}{x_{ij}},$$

$$\begin{aligned}
U_2(x_{ij}) &= 8\pi M_\pi \int \frac{d^3q}{(2\pi)^3} \frac{e^{i\vec{q}\cdot\vec{x}_{ij}/M_\pi}}{(\vec{q}^2 + M_\pi^2)^2} F_2^\Lambda(q) \xrightarrow{\Lambda\rightarrow\infty} e^{-x_{ij}}, \\
W(x_{ij}) &= \frac{1}{M_\pi^3} \int \frac{d^3q}{(2\pi)^3} e^{i\vec{q}\cdot\vec{x}_{ij}/M_\pi} F_3^\Lambda(q) \xrightarrow{\Lambda\rightarrow\infty} \delta^3(x_{ij}),
\end{aligned}
\tag{B.4}$$

where $F_{1,2,3}^\Lambda$ denotes the corresponding regulator functions.

-
- [1] P. F. Bedaque and U. van Kolck, *Ann. Rev. Nucl. Part. Sci.* **52**, 339 (2002), nucl-th/0203055.
- [2] E. Epelbaum, *Prog. Part. Nucl. Phys.* **57**, 654 (2006), nucl-th/0509032.
- [3] D. R. Entem and R. Machleidt, *Phys. Rev.* **C68**, 041001 (2003), nucl-th/0304018.
- [4] E. Epelbaum, W. Glöckle, and U.-G. Meißner, *Nucl. Phys.* **A747**, 362 (2005), nucl-th/0405048.
- [5] U. van Kolck, *Phys. Rev.* **C49**, 2932 (1994).
- [6] E. Epelbaum *et al.*, *Phys. Rev.* **C66**, 064001 (2002), nucl-th/0208023.
- [7] H. Witala *et al.*, *Phys. Rev.* **C73**, 044004 (2006), nucl-th/0601075.
- [8] S. Kistryn *et al.*, *Phys. Rev.* **C** (to appear), nucl-ex/0508012.
- [9] P. Navratil, V. G. Gueorguiev, J. P. Vary, W. E. Ormand, and A. Nogga, (2007), nucl-th/0701038.
- [10] J. Ley *et al.*, *Phys. Rev.* **C73**, 064001 (2006).
- [11] E. Epelbaum, *Phys. Lett.* **B639**, 456 (2006).
- [12] E. Epelbaum, W. Glöckle, and U.-G. Meißner, *Nucl. Phys.* **A637**, 107 (1998), nucl-th/9801064.
- [13] E. Epelbaum, *The nucleon nucleon interaction in a chiral effective field theory*, PhD thesis, Ruhr–University Bochum, Germany, 2000, JUL-3803.
- [14] S. Weinberg, *Phys. Lett.* **B251**, 288 (1990).
- [15] S. Weinberg, *Nucl. Phys.* **B363**, 3 (1991).
- [16] S. Weinberg, *Physica* **A96**, 327 (1979).
- [17] S. Weinberg, *Phys. Lett.* **B295**, 114 (1992), hep-ph/9209257.
- [18] S. Okubo, *Prog. Theor. Phys. (Japan)* **12**, 603 (1954).
- [19] V. Bernard, N. Kaiser, and U.-G. Meißner, *Int. J. Mod. Phys.* **E4**, 193 (1995), hep-ph/9501384.
- [20] V. Bernard, *Prog. Part. Nucl. Phys.* (in press), arXiv:0706.0312 [hep-ph].
- [21] E. Epelbaum, U.-G. Meißner, and W. Glöckle, *Nucl. Phys.* **A714**, 535 (2003), nucl-th/0207089.
- [22] S. N. Yang and W. Glöckle, *Phys. Rev.* **C33**, 1774 (1986).
- [23] J. A. Eden and M. F. Gari, *Phys. Rev.* **C53**, 1510 (1996), nucl-th/9601025.
- [24] S. A. Coon and J. L. Friar, *Phys. Rev.* **C34**, 1060 (1986).
- [25] J. L. Friar, *Phys. Rev.* **C60**, 034002 (1999), nucl-th/9901082.
- [26] A. V. Belitsky and T. D. Cohen, *Phys. Rev.* **C65**, 064008 (2002), hep-ph/0202153.
- [27] T. D. Cohen and B. A. Gelman, *Phys. Lett.* **B540**, 227 (2002), nucl-th/0202036.
- [28] T. D. Cohen, *Phys. Rev.* **C66**, 064003 (2002), nucl-th/0209072.
- [29] H. McManus and D. O. Riska, *Phys. Lett.* **B92**, 29 (1980).
- [30] M. R. Robilotta, *Phys. Rev.* **C31**, 974 (1985).
- [31] D. Rozpedzik *et al.*, *Acta Phys. Polon.* **B37**, 2889 (2006), nucl-th/0606017.
- [32] E. Epelbaum, U.-G. Meißner, W. Glöckle, and C. Elster, *Phys. Rev.* **C65**, 044001 (2002), nucl-th/0106007.
- [33] A. Nogga, private communication.